

2020-01

Photo- and autoxidation of unsaturated algal lipids in the marine environment: An overview of processes, their potential tracers, and limitations

Rontani, J-F

<http://hdl.handle.net/10026.1/15437>

10.1016/j.orggeochem.2019.103941

Organic Geochemistry

Elsevier BV

All content in PEARL is protected by copyright law. Author manuscripts are made available in accordance with publisher policies. Please cite only the published version using the details provided on the item record or document. In the absence of an open licence (e.g. Creative Commons), permissions for further reuse of content should be sought from the publisher or author.

Abiotic degradation of lipids in senescent phytoplanktonic cells is reviewed.

Photo- and autoxidation processes act intensively on unsaturated lipids.

Singlet oxygen plays a key role in photosensitized oxidation processes.

Autoxidation involves the reaction of triplet molecular oxygen with the substrates.

Particular attention is given to the potential of oxidation products as tracers.

1 **Photo- and autoxidation of unsaturated algal lipids in the marine environment: an**
2 **overview of processes, their potential tracers, and limitations**

3

4 Jean-François Rontani ^{a*}, Simon T. Belt ^b

5

6 ^a *Aix Marseille Univ, Université de Toulon, CNRS/INSU/IRD, Mediterranean Institute of*
7 *Oceanography (MIO) UM 110, 13288 Marseille, France*

8 ^b *Biogeochemistry Research Centre, School of Geography, Earth and Environmental*
9 *Sciences, University of Plymouth, Drake Circus, Plymouth, Devon PL4 8AA, UK*

10

11

12

13 * Corresponding author. Tel.: +33-4-86-09-06-02; fax: +33-4-91-82-96-41. *E-mail address:*

14 *jean-francois.rontani@mio.osupytheas.fr (J.-F. Rontani)*

15

16

17

18 **ABSTRACT**

19 The present paper provides an overview of results obtained in the course of recent studies
20 dealing with abiotic degradation of algal lipids in the marine realm. In the first part, the
21 photooxidation of the main lipid components (chlorophyll phytyl chain, carotenoids, Δ^5 -
22 sterols, unsaturated fatty acids, alkenones and unsaturated alkenes) in senescent
23 phytoplanktonic cells is examined. Type II photosensitized oxidation processes (i.e. involving
24 singlet oxygen) play a key role in the photooxidation of these compounds. The second part of
25 the paper describes free radical oxidation of the main lipids in senescent phytoplanktonic
26 cells. These processes, which are believed to be induced by homolytic cleavage of
27 photochemically produced hydroperoxides, involve the direct reaction of molecular oxygen in
28 its triplet ground state with organic compounds under relatively mild conditions. Particular
29 attention is given to the characterisation of pathway-specific tracers of the individual abiotic
30 reactions described. Some of these compounds appear to have the potential to provide
31 qualitative or semi-quantitative information about photooxidation, autoxidation, or the total
32 abiotic degradation state of individual or groups of organisms. On the other hand, some other
33 primary oxidation products are likely too susceptible to further degradation to permit reliable
34 quantitative estimates, but can, nonetheless, provide qualitative indication of photooxidation
35 and autoxidation.

36

37 *Keywords:* Photooxidation; Singlet oxygen; Free radical oxidation; Autoxidation; Lipids;
38 Phytoplanktonic cells; Senescence; Tracers.

39

40 **1. Introduction**

41 In order to place current trends in climate change within a context of natural variability,
42 and to better understand how Earth's climate has changed over geological time more
43 generally, it is essential to reconstruct all components of the palaeoenvironmental system
44 using a range of proxies that reflect different marine, lacustrine, terrestrial and atmospheric
45 settings. Within the marine realm, lipid biomarkers preserved in bottom sediments are
46 particularly useful for this purpose, since they represent a suitable characteristic signature of
47 sympagic (i.e. associated with sea ice) and pelagic (open water) productivity (e.g., Wakeham
48 et al., 1997; Volkman et al., 1998; Bianchi and Canuel, 2011). However, the use of lipid-
49 based approaches requires careful consideration of biomarker alteration and/or preservation
50 during their transport from the euphotic zone to the bottom sediments. It is thus critical to
51 understand how biotic and abiotic processes may alter the environmental signal encoded by
52 the biomarker proxy.

53 The majority of studies into the degradation of phytoplanktonic organic matter to date
54 have focused on biotic degradation processes (bacterial degradation, zooplanktonic grazing,
55 macrofaunal degradation) (e.g., Afi et al., 1996; Sun et al., 1999; Mäkinen et al., 2017). In
56 contrast, the role played by photochemical and free radical-mediated processes in the
57 degradation of lipid components during the senescence of phototrophic organisms has only
58 recently been investigated (Rontani et al., 2007a, 2011, 2014a,c,d; Christodoulou et al., 2010;
59 Amiraux et al., 2016). The purpose of the present paper is to provide an overview of the
60 reactions involved in such abiotic degradation processes, along with the identification of
61 suitable chemical tracers (where possible) and likely limitations that have been identified
62 during the course of these studies. Further and more detailed information can be found in the
63 cited literature throughout.

64

65 **2. Importance of lipid tracers and their oxidation products in geochemistry**

66 Proteins, carbohydrates and lipids contribute ca. 40–60%, 17–40% and 16–26%,
67 respectively, of the organic content of phytoplankton (Jónasdóttir, 2019). The different
68 phytoplankton phyla contain variable proportions of various lipid types: hydrocarbons,
69 pigments, sterols, free fatty acids, triacylglycerols, phospholipids and galactolipids. The major
70 lipid class in all the phyla are polar lipids (including phospholipids and galactolipids),
71 accounting for 40–95% of total lipids (Jónasdóttir, 2019). Due to their relative stability and
72 specificity, lipids may constitute very useful tracers of the origin of organic matter (OM).
73 Indeed, despite the generic nature of some lipid classes (e.g., saturated fatty acids, cholesterol,
74 chlorophyll), others are more specific. For example, long-chain alkenones, highly branched
75 isoprenoid (HBI) alkenes or 24-methylenecholesterol, dinosterol, long-chain alkanediols, di-
76 and triterpenoids, may be used as tracers of haptophytes, diatoms, dinoflagellates,
77 eustigmatophytes and vascular plants, respectively (see Volkman et al., 1998 for a review).

78 Moreover, identification and measurement of certain products resulting from abiotic
79 oxidation of unsaturated lipids appears to be a useful method for discerning individual
80 degradation processes such as photooxidation or autoxidation in senescent phytoplanktonic
81 cells (Rontani et al., 1998; Christodoulou et al., 2010; Amiraux et al., 2016). These
82 compounds may also provide some information on the source of the particulate or
83 sedimentary OM that is subject to different degradation processes (Rontani et al., 2012,
84 2014d, 2017). To permit quantitative estimates of abiotic lipid degradation, oxidation
85 products should ideally be sufficiently specific to the process involved (auto- or
86 photooxidation), and stable (or degraded at similar rates compared to their parent lipid) under
87 natural conditions. These criteria appear to be satisfied for the oxidation products of the
88 chlorophyll phytyl side-chain, Δ^5 -sterols and monounsaturated fatty acids, whose analysis has
89 led to quantitative estimates of the degradation state of their parent lipids in a variety of

90 natural samples (see Table 1 for details). In contrast, some other lipid oxidation products,
91 while useful from a qualitative perspective, are either too unstable or insufficiently
92 source/pathway-specific to provide quantitative information. However, it may be noted that
93 such qualitative information may still be useful for providing evidence of abiotic alteration of
94 some common palaeoenvironmental proxies (e.g., $U_{37}^{K'}$, IP₂₅, IPSO₂₅).

95

96 **3. Abiotic oxidative degradation processes**

97

98 *3.1. Photosensitized oxidation*

99

100 *3.1.1. Photooxidative reactions*

101 Direct photooxidative reactions of lipids (Zafiriou et al., 1984) are relatively rare in
102 natural environments, since very few compounds of known structure (e.g., pigments,
103 polyunsaturated fatty acids, vitamin B12, tryptophan, thiamine, etc.) possess the required
104 chromophores for photon absorption that leads to the formation of reactive excited states.
105 However, such reactions can play an important role in the photochemistry of complex organic
106 structures such as humic and fulvic acids, which do have the necessary chromophores
107 (Zafiriou, 1977). In contrast, indirect photoprocesses can be especially important in the
108 natural environment, since they can even alter those lipids whose reactive states are
109 inefficiently populated by direct light absorption (Zafiriou et al., 1984). These reactions
110 involve initial light absorption by so-called photosensitizers, which then transfer the absorbed
111 energy to other molecules, including dissolved oxygen. Within the environment, many dyes,
112 pigments and aromatic hydrocarbons are very efficient sensitizers (Foote, 1976). These
113 compounds possess two types of electronically excited states, a singlet ($^1\text{Sens}$) and a triplet
114 ($^3\text{Sens}$) (Foote, 1976), although most of the photosensitized oxidation reactions in nature

115 occur from the sensitizer in its triplet state (Gollnick, 1968). In the presence of oxygen, the
116 excited sensitizer triplet can react in two ways: (1) with another molecule directly, to give
117 radicals after hydrogen atom abstraction or electron transfer (Type I photoprocesses) (Fig. 1),
118 which react subsequently with molecular oxygen (Gollnick, 1968), or (2) with molecular
119 oxygen (Type II photoprocesses) (Fig. 1) resulting in the formation of the electronically
120 excited singlet state of oxygen ($^1\text{O}_2$), which is particularly reactive towards unsaturated
121 compounds including many lipids. Less efficient electron transfer from the triplet sensitizer to
122 oxygen leads to formation of the superoxide ion ($\text{O}_2^{\cdot-}$) (Foote, 1976).

123

124 *3.1.2. Induction of Type II photosensitized oxidation processes in senescent phototrophic* 125 *organisms*

126 Due to the presence of chlorophyll, an efficient photosensitizer (Foote, 1976; Knox and
127 Dodge, 1985), visible light-induced photosensitized processes act intensively during
128 phytoplankton senescence. Following light absorption by chlorophyll, an excited singlet state
129 (^1Chl) is formed, which, in healthy cells, is mainly used in the characteristic fast reactions of
130 photosynthesis (Foote, 1976). However, a small proportion of ^1Chl (<0.1%) undergoes
131 intersystem crossing (ISC) to form the longer-lived triplet state (^3Chl ; Knox and Dodge,
132 1985). ^3Chl is not only itself potentially damaging in Type I reactions (Fig. 2A) (Knox and
133 Dodge, 1985), but can also generate $^1\text{O}_2$, by reaction with ground state oxygen ($^3\text{O}_2$) via Type
134 II processes (Fig. 2A). Due to the susceptibility to oxidative damage of chloroplasts, there are
135 many antioxidant protective mechanisms in chloroplasts. Carotenoids quench ^3Chl and $^1\text{O}_2$ by
136 energy transfer mechanisms at very high rates (Foote, 1976) (Fig. 2A) and tocopherols can
137 remove $^1\text{O}_2$ by a quenching process and by irreversible reaction (Halliwell, 1987).

138 In senescent phototrophic organisms, the cessation of photosynthetic reactions results in
139 an accelerated rate of formation of ^3Chl and $^1\text{O}_2$ (Nelson, 1993). The rate of formation of

140 these potentially damaging species can then exceed the quenching capacity of the
141 photoprotective system and photodegradation can thus occur as a consequence (photodynamic
142 effect; Merzlyak and Hendry, 1994) (Fig. 2B).

143 The very high reactivity of $^1\text{O}_2$ with numerous membrane components (unsaturated
144 lipids, some amino acids, nucleic acids: Rontani, 2012; Devasagayam and Kamat, 2002)
145 mainly results from the loss of the spin restriction that normally hinders reaction of $^3\text{O}_2$ with
146 these biomolecules (Zolla and Rinalducci, 2002). Due to its high reactivity and short lifetime,
147 it is generally considered that $^1\text{O}_2$ is able to interact with molecules mostly in its nearest
148 environment (Krasnovsky, 1998). However, it has also been shown that $^1\text{O}_2$ produced in the
149 photosynthetic apparatus of *Chlamydomonas reinhardtii* under high light conditions is able to
150 leave the thylakoid membrane, thus reaching the cytoplasm or even the nucleus (Fisher et al.,
151 2007). The lifetime of $^1\text{O}_2$ seems thus to vary significantly in membranes according to
152 physiological conditions.

153

154 3.1.3. Photosensitized oxidation processes in the marine environment

155 In the marine environment, Type II photodegradation processes can act intensively in
156 senescent phytoplanktonic cells (Rontani, 2012). The intensity of this degradation is strongly
157 dependent on: (i) the residence time of these cells within the euphotic layer (Zafiriou et al.,
158 1984; Mayer et al., 2009), (ii) their physiological state (Nelson, 1993; Merzlyak and Hendry,
159 1994), (iii) the intensity of solar irradiance (Amiriaux et al., 2016), and (iv) the temperature
160 (Amiriaux et al., 2016). However, since the energy used by phytoplanktonic cells for growing
161 is the same employed during their photosensitized oxidation, Type II photodegradation
162 processes can act not only in surface waters but also at the level of the deep chlorophyll
163 maximum.

164 The physiological state of cells also plays a key role in the induction of Type II
165 photosensitized oxidation processes. Indeed, $^1\text{O}_2$ production can exceed the quenching
166 capacities of the photoprotective system (and thus induce cell damage) only when the
167 photosynthetic pathways are not operative, as is the case for senescent or highly stressed cells
168 (Nelson, 1993) (Fig. 2B).

169 Type II photosensitized oxidation appears to be particularly efficient in natural samples
170 in the Arctic (Rontani et al., 2012, 2016) and the Antarctic (Rontani et al., 2019a), and this
171 has been attributed to the low temperatures and solar irradiance observed in the polar regions
172 (Amiriaux et al., 2016). Although perhaps counter-intuitive, low temperatures limit the
173 diffusion of $^1\text{O}_2$ away from the membranes where it is generated (Ehrenberg et al., 1998),
174 while relatively low solar irradiances preserve the sensitizer (chlorophyll), allowing a longer
175 production time for $^1\text{O}_2$.

176

177 *3.1.4. Type II photosensitized oxidation of the main unsaturated lipids in senescent algae*

178

179 *3.1.4.1. Chlorophylls*

180 Phytoplankton contain a large number of different pigments, the most important of them
181 being chlorophylls (Jeffrey et al., 1997). Irradiation of dead phytoplankton cells by
182 photosynthetically active radiation (PAR) and ultraviolet radiation (UVR) results in rapid
183 degradation of chlorophylls (Nelson, 1993; Rontani et al., 1995; Christodoulou et al., 2010).
184 Despite some progress identifying intermediate photoproducts (Engel et al., 1991; Iturraspe et
185 al., 1994), no stable and specific markers for the photodegradation of the chlorophyll
186 macrocycle have yet to be characterised. However, the isoprenoid phytol side-chain of
187 chlorophylls (**1**), which is photodegraded 3–5 times slower than the chlorophyll tetrapyrrolic
188 structure (Cuny et al., 1999; Christodoulou et al., 2010), undergoes Type II photosensitized

189 oxidation leading to the production of photoproducts **a** and **b** (Fig. 3). Such oxidation
190 products are identifiable and quantifiable following NaBH₄ reduction and alkaline hydrolysis
191 to yield 6,10,14-trimethylpentadecan-2-ol (**2**) and 3-methylidene-7,11,15-trimethyl-
192 hexadecan-1,2-diol (phytyldiol) (**3**), respectively (Fig. 3) (Rontani et al., 1994).

193 Phytyldiol (**3**), which is ubiquitous in the marine environment and results specifically
194 from the action of ¹O₂, has been proposed as specific tracer for photodegradation of the
195 chlorophyll phytyl side-chain (Rontani et al. 1994, 1996; Cuny and Rontani, 1999).
196 Furthermore, the molar ratio phytyldiol:phytol (Chlorophyll Phytyl side-chain
197 Photodegradation Index, CPPI) has been proposed to estimate the extent of photodegraded
198 chlorophyll in situ using the empirical Eqn. 1 (Cuny et al. 2002). Quantification of phytol (**1**)
199 and phytyldiol (**3**) has thus led to quantitative estimates of chlorophyll photooxidation
200 percentages in various natural samples including suspended and sinking particles from
201 tropical and temperate settings and the polar regions (Table 1). Such estimates range from 0 to
202 100%, indicating complete photooxidation of chlorophyll in several cases.

$$203 \text{ Chlorophyll photodegradation \%} = (1 - (\text{CPPI} + 1)^{-18.5}) \times 100 \quad (\text{Eqn. 1})$$

204

205 *3.1.4.2. Carotenoids*

206 Carotenoids are widely distributed in marine and freshwater phytoplankton (for a
207 review see Huang et al., 2017). Some carotenoids are found only in specific algal divisions or
208 classes; therefore, these compounds are often used as chemotaxonomic markers (Takaichi,
209 2011). As important components of the photoprotective system of phytoplanktonic cells,
210 carotenoids occur in close molecular-scale association with chlorophylls, even when the
211 structure of the thylakoid membrane has been disrupted (Nelson, 1993). Thus, during the
212 senescence of these organisms, when the production of ¹O₂ exceeds their quenching capacity,
213 carotenoids can be strongly affected by Type II photosensitized oxidation processes. For

214 example, loliolide (**4**) and *iso*-loliolide (**5**) (Fig. 4), which are produced during Type II
215 photosensitized oxidation of carotenoids (Iseo et al., 1972), were previously detected in
216 senescent cells of *Dunaliella* sp. following irradiation by visible light (Rontani et al., 1998).
217 However, due to their apparent additional production by anaerobic bacteria (Repeta, 1989)
218 and during dark incubations of senescent phytoplanktonic cells (Rontani et al., 1998), these
219 compounds do not constitute unequivocal indicators of Type II photosensitized oxidation of
220 carotenoids.

221

222 3.1.4.3. Δ^5 -sterols

223 In phytoplanktonic cells, Δ^5 -sterols are important membrane components that stabilize
224 the structure of phospholipid bilayers and thus play a significant role in membrane
225 temperature acclimation (Piepho et al., 2012). Moreover, they are important precursors for
226 steroid hormones (Goad, 1981). These unsaturated components of biological membranes
227 contribute ca. 2–8% of the lipid pool of the different phyla (Jónasdóttir, 2019) and are highly
228 susceptible to photooxidative degradation during the senescence of phytoplankton. Type II
229 photosensitized oxidation of these compounds mainly produces Δ^6 -5 α -hydroperoxides (**6**) and
230 to a lesser extent Δ^4 -6 α /6 β -hydroperoxides (**7** and **8**; Fig. 5) (Nickon and Bagli, 1961; Kulig
231 and Smith, 1973; Korytowski et al., 1992). Δ^6 -5 α -hydroperoxides (**6**) are relatively unstable
232 and commonly undergo allylic rearrangement to Δ^5 -7 α -hydroperoxysterols (**9**), which in turn
233 epimerize to the corresponding 7 β -hydroperoxides (**10**; Fig. 5) (Smith, 1981).

234 Irradiation by visible light of senescent cells of several phytoplankton species (Rontani
235 et al., 1997a, 1997b, 1998) resulted in rapid photodegradation of the main Δ^5 -sterols of these
236 algae, as shown by the identification of the alcohols corresponding to the hydroperoxides **7**–
237 **10** following NaBH₄ reduction and alkaline hydrolysis.

238 Although produced in lower relative amounts compared to the Δ^6 -5 α -hydroperoxides
239 **(6)**, the more stable and specific Δ^4 -6 α /6 β -hydroperoxides (**7** and **8**), quantified after NaBH₄
240 reduction to the corresponding Δ^4 -stera-6 α /6 β -diols **11** and **12** (Fig. 5), have been proposed as
241 more reliable tracers of Type II photosensitized oxidation of Δ^5 -sterols. Further, the extent of
242 photooxidation (%) of the parent sterol can be estimated from the relative proportions of Δ^6 -
243 5 α -hydroperoxides (**6**) and Δ^4 -6 α /6 β -hydroperoxides (**7** and **8**) observed in biological
244 membranes (ratio $(\mathbf{7} + \mathbf{8})/\mathbf{6} \approx 0.3$, Korytowski et al., 1992; Christodoulou et al., 2009; Rontani
245 et al., 2009) using Eqn. 2. Using this approach, the photooxidation state (%) of several Δ^5 -
246 sterols in suspended and sinking particles, sea ice, sediments and terrestrial plants from a
247 range of locations have been estimated (Table 1). Interestingly, the photooxidation state of
248 these compounds appears to be greatest at high latitudes; this may be attributed to the low
249 temperatures observed in such regions, a factor that is well-known to decrease the diffusion
250 rate of ¹O₂ outside of cell membranes (Ehrenberg et al., 1998). Further, due to the source-
251 specificity of some Δ^5 -sterols (Volkman, 1986, 2003), their oxidation products can also
252 provide interesting information about the photooxidation state of specific phyla of
253 phytoplankton (e.g., diatoms, haptophytes or chlorophytes; Rontani et al., 2012a, 2016,
254 2019a) or terrestrial higher plants (Rontani et al., 2014d). For example, photodegradation
255 processes appears to act more intensively on 24-methylenecholesterol (mainly arising from
256 diatoms; Volkman, 1986, 2003) (photooxidation percentages ranging from 10 to 40% in the
257 Antarctic; Rontani et al., 2019a) than on *epi*-brassicasterol (arising from diatoms and/or
258 haptophytes; Volkman, 1986, 2003) (photooxidation percentages ranging from 3 to 15% in
259 the same samples). Type II photosensitized oxidation processes therefore seem to be more
260 efficient in diatoms compared to haptophytes, although the reason for this remains to be
261 elucidated.

262

263 Δ^5 -sterol photooxidation % = (Δ^4 -stera-6 α / β -diols % \times (1 + 0.3)/0.3) (Eqn. 2)

264

265 *3.1.4.4. Unsaturated fatty acids*

266 Fatty acids constitute the building block of the main lipid types of the phytoplankton
267 (triacylglycerols, galactolipids and phospholipids; Jónasdóttir, 2019). Unsaturated fatty acids
268 (including monounsaturated (MUFAs) and polyunsaturated (PUFAs) acids), ranging from 45
269 to 85% of the total fatty acids in the different phytoplankton groups (Jónasdóttir, 2019), are
270 particularly susceptible to Type II photooxidation (Heath and Packer, 1968). Type II
271 photosensitized oxidation of MUFAs involves a direct reaction of $^1\text{O}_2$ with the carbon-carbon
272 double bond by a concerted ‘ene’ addition (Frimer, 1979) and leads to formation of
273 hydroperoxides at each end of the original double bond (Fig. 6). These hydroperoxides, each
274 with an allylic *trans*-double bond (Frankel et al., 1979; Frankel, 1998), can subsequently
275 undergo stereoselective radical allylic rearrangement affording two other isomers with a *trans*
276 double bond (Fig. 6; Porter et al. 1995). Isomeric *trans* allylic hydroxyacids resulting from
277 NaBH_4 reduction of these photoproducts may thus be used as tracers of Type II
278 photosensitized oxidation of MUFAs. However, this requires subtraction of the amounts of
279 these compounds arising from autoxidation (See Section 4.3.3).

280 Using this approach, photoproducts of MUFAs were detected previously in senescent
281 cells of phytoplanktonic algae (Marchand and Rontani, 2001; Christodoulou et al., 2010;
282 Amiraux et al., 2016) and in several natural samples (Table 1). As in the case of sterols (see
283 Section 3.1.4.3.), photooxidation of MUFAs appears to be especially significant in the polar
284 regions. On the basis of the high photooxidation percentages (up to 100%) of MUFAs
285 measured in various samples of suspended and sinking particles (Table 1), and the well-
286 known increasing photooxidation rates of fatty acids with their degree of unsaturation
287 (Frankel, 1998; Rontani et al., 1998), a strong photooxidation of PUFAs in the marine

288 environment would be expected. However, photooxidation products of PUFAs have not been
289 detected in natural samples, likely due to their instability with respect to further reactions,
290 including secondary oxidation.

291

292 3.1.4.5. Alkenones

293 Alkenones are a class of mono-, di-, tri-, tetra- and penta-unsaturated C₃₅–C₄₀ methyl
294 and ethyl ketones (Boon et al., 1978; Volkman et al., 1980, 1995; de Leeuw et al., 1980;
295 Marlowe et al., 1984; Prahl et al., 2006; Jaraula et al., 2010), which are produced by certain
296 marine haptophytes. The unsaturation ratio of C₃₇ alkenones is defined by Eqn. 3, where
297 [C_{37:2}] and [C_{37:3}] are the concentrations of di- and tri-unsaturated C₃₇ alkenones respectively,
298 and varies positively with the growth temperature of the alga (Prahl and Wakeham, 1987;
299 Prahl et al., 1988).

$$300 \quad U_{37}^{K'} = [C_{37:2}] / ([C_{37:2}] + [C_{37:3}]) \quad (\text{Eqn. 3})$$

301 The $U_{37}^{K'}$ index is thus now used routinely for paleotemperature reconstructions (e.g.,
302 Brassell et al., 1986; Prahl and Wakeham, 1987; Brassell, 1993; Müller et al., 1998). Visible
303 light-induced photodegradation of these compounds was previously investigated in order to
304 determine if photochemical processes acting selectively on C_{37:2} and C_{37:3} alkenones could
305 appreciably modify $U_{37}^{K'}$ ratios during algal senescence (Rontani et al., 1997b; Mouzdahir et
306 al., 2001; Christodoulou et al., 2010).

307 Type II photosensitized oxidation of alkenones is not sufficiently rapid in dead cells of
308 haptophytes to induce strong modification of the $U_{37}^{K'}$ ratio before the photo-destruction of the
309 photosensitizing substances (Rontani et al., 1997b; Mouzdahir et al., 2001; Christodoulou et
310 al., 2010). This poor reactivity was attributed to: (i) the *trans* geometry of the alkenone double
311 bonds (Rechka and Maxwell, 1988), which is 7–10 times less sensitive to Type II
312 photosensitized oxidation than the *cis* configuration of fatty acids (Table 2) (Hurst et al.,

313 1985), (ii) the separation of the double bonds by five carbons in the alkenone structure instead
314 of one in the case of PUFAs, or (iii) the occurrence of these compounds in cytoplasmic
315 vesicles (Eltgroth et al., 2005), which could significantly decrease the frequency of interaction
316 between $^1\text{O}_2$ and alkenones, even if there are indications that $^1\text{O}_2$ should easily diffuse into
317 such microenvironments (Christodoulou et al., 2010).

318

319 3.1.4.6. *n*-Alkenes

320 It was previously established that the hydrocarbon fraction of the eustigmatophyte
321 *Nannochloropsis salina* contained C_{25} , C_{27} and C_{29} polyunsaturated *n*-alkenes (Gelin et al.,
322 1997). C_{37} and C_{38} *n*-alkenes with 2, 3 and 4 double bonds could also be detected in the
323 haptophytes *Emiliania huxleyi* CS-57 (Volkman et al., 1980). C_{31} and C_{33} *n*-alkenes were also
324 present in this strain but in smaller amounts. Type II photosensitized oxidation of *n*-alkenes
325 was previously investigated in senescent cells of *E. huxleyi* and *N. salina* (Mouzdahir et al.,
326 2001). In the former, minor C_{31} and C_{33} *n*-alkenes possessing *cis* double bonds (Rieley et al.,
327 1998) were strongly photodegraded, while major C_{37} and C_{38} *n*-alkenes possessing *trans*
328 internal double bonds (Rieley et al., 1998) appeared particularly recalcitrant towards
329 photochemical processes. As seen with alkenones, the photochemical recalcitrance of C_{37} and
330 C_{38} *n*-alkenes was partly attributed to the well-known poor reactivity of $^1\text{O}_2$ with *trans* double
331 bonds (Table 2) (Hurst et al., 1985). However, a localisation of these alkenes outside of the
332 main membranes (e.g., cytoplasmic vesicles; Eltgroth et al., 2005) could also play a role in
333 their weak photooxidative reactivity.

334 Visible light irradiation of dead cells of *N. salina* showed no significant light-dependent
335 degradation of monounsaturated hydrocarbons. This observation was attributed to the terminal
336 position of the double bond in these compounds (Gelin et al., 1997), which is poorly reactive
337 towards $^1\text{O}_2$ (Table 2) (Kopecky and Reich, 1965). In contrast, di-, tri-, and tetraenes were

338 strongly photodegraded during irradiation, with their degradation rates increasing
339 systematically with the number of double bonds, as expected.

340

341 3.1.4.7. HBI alkenes

342 C₂₅ and C₃₀ Highly branched isoprenoid (HBI) alkenes, sometimes referred to as
343 haslenes and rhizenes, respectively, are produced by a relatively small number of marine and
344 freshwater diatoms. To date, haslenes have been reported in species belonging to the
345 *Berkeleya*, *Haslea*, *Navicula*, *Pleurosigma*, *Pseudosolenia* and *Rhizosolenia* genera, while the
346 only known source of rhizenes is *R. setigera* (Volkman et al., 1994; Belt et al., 1996, 2000,
347 2001; Sinninghe Damsté et al., 1999, 2004; Brown et al., 2014; Brown and Belt, 2016; Kaiser
348 et al., 2016). C₂₅ HBI alkenes (exhibiting 1–6 double bonds) are the most commonly reported
349 HBIs in marine sediments (Rowland and Robson, 1990; Belt et al., 2000). Despite their
350 common occurrence, however, relatively little attention has been given to their use as
351 palaeoenvironmental proxies, which is perhaps surprising given their apparent source-
352 specificity. Exceptions to this can be found in the polar regions, where 3,9,13-trimethyl-6-
353 (1,5-dimethylhexyl)-tetradec-1-ene (**19**) (referred as IP₂₅) and 2,6,10,14-tetramethyl-7-(3-
354 methylpent-4-enyl)-pentadec-6(17)-ene (**20**) (referred as IPSO₂₅) (Fig. 7) have been proposed
355 as proxy measures of past seasonal sea ice in the Arctic and Antarctic, respectively (Belt et
356 al., 2007, 2016; Belt, 2018). Furthermore, among the main polyunsaturated HBIs **21–24** (Fig.
357 7), the tri-unsaturated HBI **22**, which is produced by certain pelagic diatoms including *R.*
358 *setigera* (Belt et al., 2017), has been identified as a potentially useful open-water counterpart
359 to IP₂₅ when using the so-called PIP₂₅ index for calculating semi-quantitative sea ice estimates
360 (see Belt, 2018 for a recent review). Furthermore, **22** and its diastereoisomer (HBI **23**) (Fig. 7)
361 have been proposed as possible proxies for the marginal ice zone in the polar regions (Belt et
362 al., 2015; Belt, 2018; Köseoğlu et al., 2018a,b), while the ratio between them (expressed as

363 **22/(22+23)**; HBI TR₂₅) has recently been suggested as a proxy measure for the spring
364 phytoplankton bloom, at least in northern high latitudes (Belt et al., 2019).

365 In order to compare the efficiency of type II photosensitized oxidation processes upon
366 HBI alkenes and other well-known phytoplanktonic lipids, solutions of a mixture of mono-,
367 di-, tri- and tetraunsaturated HBI alkenes (**19–29**), methyl oleate (**30**) (as a model of
368 glycerides), phytyl acetate (**31**) (as a model of chlorophyll phytyl side-chain), cholesteryl
369 acetate (**32**) (as a model of esterified sterols) and vitamin E (**13**) were irradiated in the
370 presence of hematoporphyrin as sensitizer (Rontani et al., 2011). Interestingly, while the
371 reactivity of fatty acids towards ¹O₂ increases with their degree of unsaturation (Frankel,
372 1998), the reactivity of HBI alkenes towards ¹O₂ was found to be most dependent on the
373 number of tri-substituted double bonds (Table 3). Indeed, the rate of the ene reaction of ¹O₂
374 with alkenes, which is controlled by activation entropy (Hurst et al., 1985), increases strongly
375 with the degree of substitution of the double bond (Table 2). As a consequence, IP₂₅ (**19**),
376 containing only a terminal double bond, and IPSO₂₅ (**20**), containing a terminal double bond
377 and a methylidene group, reacted much slower with ¹O₂ than their tri-unsaturated counterparts
378 (Table 3) (Rontani et al., 2011). In contrast, HBI trienes and tetraenes with at least one tri-
379 substituted double bond were photodegraded at similar or higher rates compared to vitamin E
380 (**13**), which is well-known to be very reactive towards ¹O₂ (Yamauchi and Matsushita, 1979;
381 Clough et al., 1979; Nassiry et al., 2009) (Table 2). Although HBI triene **21**, phytyl acetate
382 (**31**) and cholesteryl acetate (**32**) all contain a tri-substituted double bond, the following order
383 of photoreactivity was observed: triene **21** > phytyl acetate (**31**) > cholesteryl acetate (**32**)
384 (Table 3). These differences in reactivity were attributed to: (i) electronic deactivation of the
385 double bond in phytyl acetate (**31**) by the electron accepting acetoxy group at the allylic
386 position (Griesbeck et al., 2003) and (ii) steric hindrance between the sterol Δ⁵ double bond
387 and ¹O₂ (Beutner et al., 2000). The lower reactivity of HBI **22** and **23** possessing two tri-

388 substituted double bonds (compared to HBI **21**) towards singlet oxygen (Table 2) was also
389 attributed to their enhanced rigidity or steric hindrance resulting from the presence of the 7-20
390 double bond (Rontani et al., 2014a). Photodegradation of HBI alkenes and other lipids was
391 also compared in dead cells of the diatom *Haslea ostrearia* (Rontani et al., 2011) and HBIs
392 with at least one tri-substituted double bond were photodegraded at comparable or higher
393 rates compared to chlorophyll a.

394 In the case of HBI trienes **22** and **23**, photooxidation appeared to occur exclusively at
395 the tri-substituted 9-10 and 7-20 double bonds. Since *syn* ene addition of $^1\text{O}_2$ at the more
396 crowded side of tri-substituted double bonds is strongly favoured (Orfanopoulos et al., 1989),
397 reaction between $^1\text{O}_2$ and the 9-10 and 7-20 double bonds in **22** and **23** should result mainly in
398 the formation of allylic hydroperoxides **33–38** (Fig. 8). Reduction products of compounds **34**
399 and **35** could not be detected among photoproducts of trienes **22** and **23**, likely due to the very
400 high reactivity of conjugated dienic systems toward $^1\text{O}_2$ (Frimer, 1983) inducing a very fast
401 conversion to labile endoperoxides. Quantitatively, the alcohols **39–42** obtained after NaBH_4
402 reduction of the corresponding hydroperoxides **33** and **36–38** represented only a very small
403 proportion of the substrate degraded (Rontani et al., 2014a), attributed to rapid secondary
404 reactions of the four primary photoproducts.

405 Since compounds **40–42** can also be produced by autoxidation (see Section 4.3.5.), only
406 compound **39** has been proposed as a specific (and qualitative) tracer of HBI alkene
407 photooxidation (Fig. 8) (Rontani et al., 2014a). Interestingly, compound **39** could be detected
408 in sea ice samples from the Arctic (Rontani et al., 2014b) and in weakly oxidized
409 phytoplankton from Antarctica (Rontani et al., 2019a), thus confirming the vulnerability of
410 HBI trienes **22** and **23** towards Type II photosensitized oxidation under environmental
411 conditions. Unfortunately, the lability (resulting from further oxidation) of this tracer
412 prevented more quantitative photooxidation estimates from being made.

413

414 3.1.4.8. Vitamin E

415 Vitamin E (**13**) is relatively abundant in most photosynthetic organisms and notably in
416 microalgae (Brown et al., 1999). As an important constituent of the photoprotective system of
417 the cells, vitamin E (**13**) reacts very efficiently with $^1\text{O}_2$ affording mainly 8a-
418 hydroperoxycopherone (**14**) (Yamauchi and Matsushita, 1979; Clough et al., 1979) (Fig. 9).
419 Heterolytic and homolytic degradation of compound **14** affords different isoprenoid products
420 (4,7,12-trimethyltridecanoic acid (**15**), 6,10,14-trimethylpentadecan-2-one (**16**), 4,8,12,16-
421 tetramethylheptadecan-4-olide (**17**) and α -tocopherylquinone (**18**)) (Nassiry et al., 2009) (Fig.
422 9). Unfortunately, peroxy radicals also react with the 8a position of vitamin E (**13**) to form
423 compound **14** (Liebler, 1994) (Fig. 9), thereby making it difficult to differentiate between
424 photo- and autoxidation reactions. It is interesting to note, however, that the main oxidation
425 products of vitamin E (**13**) are trimeric compounds, which seem to be a potential source of
426 pristane in sediments (Rontani et al., 2010).

427

428 3.1.4.9. Kinetic aspects

429 First-order kinetics generally adequately describe the Type II photosensitized oxidation
430 of lipid components of senescent phytoplanktonic cells (Nelson, 1993; Rontani et al., 1998).
431 However, an exception could be observed in the case of *n*-alkenes present in *N. salina* whose
432 photodegradation seems to be a second-order process (Mouzdahir et al., 2001). Half-life doses
433 of the main lipid components of phytoplanktonic cells are summarized in Table 4. On the
434 basis of the different photodegradation rate constants measured in different studies, the
435 following order of photoreactivity of phytoplanktonic lipids can be proposed: HBIs with tri-
436 substituted double bonds \approx chlorophylls \approx polyunsaturated fatty acids and *n*-alkenes \approx
437 carotenoids $>$ MUFAs \approx chlorophyll phytyl side-chain $>$ Δ^5 -sterols $>$ alkenones $>$ IP₂₅.

438

439 **4. Free radical oxidation (autoxidation)**

440

441 *4.1. Induction of autoxidation processes in senescent phototrophic organisms*

442 In contrast to photooxidation, autoxidation involves the direct reaction of molecular
443 oxygen in its triplet ground state (i.e. $^3\text{O}_2$) with organic compounds under relatively mild
444 conditions. Autoxidation can be described as a free-radical-mediated oxidation chain-reaction
445 and can be divided into three major steps: chain initiation, propagation and termination (Fig.
446 10). The mechanisms of initiation of lipid oxidation have been debated for many years. In
447 senescent phytoplanktonic cells, initiation seems to result from the decomposition of
448 hydroperoxides produced during photodegradation of cellular organic matter (Girotti, 1998;
449 Rontani et al., 2003). During the initiation phase, the generation of radicals can result from the
450 involvement of enzymes (e.g., lipoxygenases (LOXs)), redox-active metal ions undergoing
451 one-electron transfer, heat or light (Fig. 10) (Sheldon and Kochi, 1976; Schaich, 2005).
452 Redox-active metal ions (e.g., Co^{2+} , Fe^{2+} , Fe^{3+} , Cu^{2+} , Mn^{2+} , Zn^{2+} , Mg^{2+} , V^{2+}) are generally
453 considered as the initiators of highest importance for lipid oxidation in biological systems
454 (Pokorny, 1987; Schaich, 2005) and can direct the cleavage of hydroperoxides either through
455 alkoxy or peroxy radicals (Fig. 10). The well-known generation of radicals in the course of
456 the LOX catalytic cycle may also act like a catalyst in autoxidation (Fuchs and Spiteller,
457 2014). Moreover, when LOX activity becomes very high, increasing amounts of free radicals
458 may damage the active site of LOXs and release Fe^{2+} ions (Sato et al., 1992; Fuchs and
459 Spiteller, 2014). Peroxy and alkoxy radicals thus formed can then abstract a hydrogen atom
460 from a relatively weak C–H bond (e.g., allylic, tertiary, α to oxygen; Fossey et al., 1995) or
461 add to an unsaturated system, inducing a radical chain-reaction (Fig. 10). The chain-reaction

462 ends when free radicals combine to form a new bond, hence rendering them unreactive (Fig.
463 10).

464 Free radical oxidation processes play a pivotal role in the deleterious effects of
465 senescence in plants (Leshem, 1988). Further, it has been demonstrated that viral infection
466 (Evans et al., 2006) and autocatalytic programmed cell death (Bidle and Falkowski, 2004) of
467 phytoplanktonic cells can also lead to elevated production of reactive oxygen species (ROS)
468 able to induce the radical degradation of cell components.

469

470 *4.2. Autoxidation processes in the marine environment*

471

472 While the effects of Type II photosensitized oxidation processes in phytodetritus are
473 limited to the euphotic layer of the oceans, autoxidation processes can act on such material
474 not only throughout the water column, but also in the oxic layer of sediments. It is generally
475 considered that the rate and extent of autoxidation of sedimentary organic compounds is
476 strongly dependent on the molecular structure of the substrate, protective effects offered by
477 association of organic matter with particle matrices, and the length of time accumulating
478 particles are exposed to molecular oxygen in sedimentary pore waters (Henrich, 1991;
479 Hartnett et al., 1998). Autoxidation should thus be especially prevalent in cases where
480 sequestered algal material experiences long residence times in the oxic layer of sediments.

481 Even though autoxidation is a very well-known chemical process, its significance in
482 environmental studies has only relatively recently been demonstrated (Christodoulou et al.,
483 2009; Rontani et al., 2009, 2014c, 2017; Galeron et al., 2018).

484

485 *4.3. Autoxidation of the main unsaturated lipids in senescent algae*

486

487 4.3.1. Chlorophylls

488 Chlorophyll allomers such as 13²-hydroxychlorophyll a (HO-chl-a) (**43**) and 13²-
489 methoxychlorophyll a (MeO-chl-a) (**44**) (Fig. 11) are thought to be formed by autoxidation
490 through reaction with ground state oxygen (Hynninen, 1991). HO-chl-a has been found in
491 senescent and virally infected cultures (Bale et al., 2013), while HO-chl-a (**43**) and MeO-chl-a
492 (**44**) have both been shown to increase in *Thalassiosira pseudonana* cultures at the onset of
493 senescence (Franklin et al., 2012). However, very little is known about the formation of
494 allomers during phytoplankton mortality, and additional culture studies are required to test the
495 ubiquity or specificity of allomer formation (Walker and Keely, 2004).

496 Autoxidation of the esterified chlorophyll phytyl chain involves either addition of
497 peroxy radicals to the double bond or hydrogen abstraction at the allylic carbon 4 (Fig. 12)
498 (Rontani and Aubert, 1994, 2005). Addition of a peroxy radical to the double bond affords a
499 tertiary radical, which can then: (i) lead to epoxides by fast intramolecular homolytic
500 substitution (Fossey et al., 1995), or (ii) react with molecular oxygen, which after hydrogen
501 abstraction from another molecule of substrate, yields a diperoxide (Fig. 12). Following
502 NaBH₄ reduction and alkaline hydrolysis, these compounds are converted to 3,7,11,15-
503 tetramethylhexadecan-1,2,3-triol (**45**) (Fig. 12). Abstraction of a hydrogen atom from C-4 and
504 subsequent oxidation of the allylic radicals thus formed yields four isomeric hydroperoxides,
505 which are converted (after NaBH₄ reduction and alkaline hydrolysis) to *Z* and *E* 3,7,11,15-
506 tetramethylhexadec-3-en-1,2-diols (**46** and **47**) and *Z* and *E* 3,7,11,15-tetramethyl-hexadec-2-
507 en-1,4-diols (**48** and **49**) (Fig. 12). Recently, autoxidative conversion of the chlorophyll phytyl
508 side-chain to isophytol (**50**) has also been observed (Rontani and Galeron, 2016) and
509 attributed to allylation (Berkessel, 2014) of the phytyl side-chain by peroxy radicals (Rontani
510 et al., 2019a) (Fig. 12). Compounds **46–49**, which are widespread in the marine environment,
511 therefore constitute useful and specific tracers of chlorophyll autoxidation. Unfortunately, the

512 well-known biotic and abiotic lability of epoxides in sediments (Rontani et al., 2019b) and
513 during sample treatment (due to formation of methoxyhydrins and chlorohydrins; Marchand
514 and Rontani, 2001) (Fig. 12) precludes quantitative estimates of chlorophyll phytyl side-chain
515 autoxidation.

516

517 4.3.2. Δ^5 -sterols

518 Free radical oxidation of Δ^5 -sterols yields mainly 7α - and 7β -hydroperoxides and, to a
519 lesser extent, $5\alpha/\beta,6\alpha/\beta$ -epoxysterols and $3\beta,5\alpha,6\beta$ -trihydroxysterols (Smith, 1981; Morrissey
520 and Kiely, 2006) (Fig. 13). 7-Hydroperoxysterols, which may be also formed by allylic
521 rearrangement of photochemically produced 5α -hydroperoxysterols (see Section 5.1.4.3) are
522 not sufficiently specific and stable to be used as tracers of Δ^5 -sterol autoxidation. Although
523 more specific, $5\alpha/\beta,6\alpha/\beta$ -epoxysterols are not stable enough to be used as tracers. Indeed, they
524 may be easily hydrolysed to the corresponding triol in seawater and during the treatment of
525 the samples (Fig. 13). $3\beta,5\alpha,6\beta$ -Trihydroxysterols have therefore been identified as suitable
526 tracers of sterol autoxidation. Furthermore, the extent of sterol autoxidation can be estimated
527 (Eqn. 4) using rate constants previously obtained from incubation experiments (Morrissey and
528 Kiely, 2006; Rontani et al., 2014c). The autoxidation state of some algal and higher plant Δ^5 -
529 sterols has thus been estimated in various natural samples including suspended and sinking
530 particles, sea ice and sediments (Table 1). The high values observed (up to 90%) attest to the
531 efficiency of autoxidative processes in the marine realm. It may be noted, however, that the
532 relatively poor chromatographic properties of the only partially silylated $3\beta,5\alpha,6\beta$ -
533 trihydroxysterols (at positions 3 and 6) may hinder autoxidation estimates at low
534 concentrations (Rontani et al., 2019a).

$$535 \text{ Sterol autoxidation \%} = 3\beta,5\alpha,6\beta\text{-Trihydroxysterol \%} \times 2.4 \quad \text{Eqn. 4}$$

536

537 4.3.3. Unsaturated fatty acids

538 Autoxidation of MUFAs mainly involves allylic hydrogen abstraction and subsequent
539 oxidation of the allylic radical thus formed, yielding 6 isomeric allylic hydroperoxyacids (Fig.
540 14). Free radical oxidative processes can be readily characterised after NaBH₄ reduction based
541 on the presence of *cis* allylic hydroxyacids, which are not produced photochemically (see Fig.
542 6), and are specific products of these degradation processes (Porter et al., 1995; Frankel,
543 1998). The proportion of *trans* hydroxyacids resulting from autoxidative processes may be
544 distinguished from that arising from photooxidative processes according to the proportions of
545 *cis* hydroxyacids detected and the ambient temperature (°C) (see Eqns. 5–8 in the case of Δ⁹
546 MUFAs) (Frankel 1998; Marchand and Rontani 2001). Autoxidation percentages are obtained
547 from the ratio of the sum of measured *cis* and calculated *trans* autoxidative allylic
548 hydroxyacids to the parent MUFA.

$$549 \frac{[8-cis] + [11-cis]}{[9-trans]} = -0.0138T + 1.502 \quad (\text{Eqn. 5})$$

$$550 \frac{[8-cis] + [11-cis]}{[10-trans]} = -0.0144T + 1.553 \quad (\text{Eqn. 6})$$

$$551 \frac{[8-cis]}{[8-cis] + [8-trans]} = -0.0055T + 0.627 \quad (\text{Eqn. 7})$$

$$552 \frac{[11-cis]}{[11-cis] + [11-trans]} = -0.0055T + 0.627 \quad (\text{Eqn. 8})$$

553 Oxidation products of MUFAs have proven to be very sensitive markers of individual
554 photooxidation and autoxidation pathways, especially during phytoplankton growth, with low
555 amounts of degradation products corresponding to bloom events and high amounts
556 corresponding to pre- and post-bloom periods (Christodoulou et al., 2009).

557 Despite the strong autoxidation percentages of MUFAs measured in various natural
558 samples (up to 100%) (Table 1) and the increasing rates of autoxidation of fatty acids with the
559 degree of unsaturation (Frankel, 1998), autoxidation products of PUFAs have thus far not be
560 detected in senescent phytoplanktonic cells. This is possibly due to the instability of the
561 hydroperoxides formed, or the involvement of cross-linking reactions, which lead to the

562 formation of macromolecular structures (Neff et al., 1988) that are not amenable for analysis
563 by gas chromatographic methods.

564

565 4.3.4. Alkenones

566 Alkenones appear to be more sensitive towards oxidative free radical processes than
567 other common marine lipids such as phytol acetate (**31**), methyl oleate (**30**) and cholesteryl
568 acetate (**32**), and their oxidation rates increase proportionally with their unsaturation (Rontani
569 et al., 2006). As a consequence, these abiotic degradation processes have the potential to
570 significantly increase (up to 0.20) the $U_{37}^{K'}$ ratio and thus bias alkenone-based
571 paleotemperature estimations towards higher temperatures (up to +5.9°C).

572 Autoxidation of alkenones involves mainly allylic hydrogen abstraction and subsequent
573 oxidation of the allylic radical thus formed. Oxidation of each double bond and subsequent
574 NaBH₄ reduction thus affords four positional isomeric alkenediols (Fig. 15). Unfortunately,
575 these compounds, which could be very useful tracers of autoxidation of alkenones, are not
576 accumulated. Indeed, due to the presence of additional reactive double bonds,
577 hydroperoxyalkenones undergo subsequent oxidation reactions to produce di-, tri- and
578 tetrahydroperoxyalkenones, according to the degree of unsaturation of the starting alkenone
579 (Rontani et al., 2013). However, the reduction products are not amenable for analysis using
580 standard gas chromatographic methods. Interestingly, alkenediols resulting from post-
581 extraction NaBH₄ reduction of the corresponding hydroperoxyalkenones (Fig. 15), have been
582 observed in cultures of *E. huxleyi* (strain CS-57) that exhibited anomalously high $U_{37}^{K'}$ values
583 (Rontani et al., 2007a) and a further strain (TWP1) maintained in the dark (Rontani et al.,
584 2013). These compounds were also detected in sediments from southeast Alaska (Rontani et
585 al., 2013) (Table 1).

586

587 4.3.5. HBI alkenes

588 The relative rates of autoxidation of various HBI alkenes was investigated by taking
589 mixtures of mono-, di-, tri- and tetra-unsaturated HBI alkenes **19–25**, methyl oleate (**30**),
590 phytyl acetate (**31**) and cholesteryl acetate (**32**) in hexane and incubating in the presence of a
591 radical enhancer (*tert*-butyl hydroperoxide) and a radical initiator (*di-tert*-butyl nitroxide)
592 (Porter et al., 1995; Rontani et al., 2014a). Consistent with the general increase in
593 autoxidation rate with unsaturation seen with other lipids (Frankel, 1998), the following order
594 of reactivity was observed: IP₂₅ < IPSO₂₅ < HBI triene **21** < HBI tetraene **25** < HBI trienes **22**
595 and **23** (Table 5) (Fig. 7). The highest degradation rates of trienes **22** and **23** was attributed to
596 the presence of a very reactive bis-allylic methylene group (C-8) (Fig. 7) that can lose a
597 hydrogen atom very readily. Indeed, it was previously estimated that the rate of hydrogen
598 abstraction for bis-allylic positions is in the region of 60 times higher than for their mono-
599 allylic counterparts (Ingold, 1969). Incubation of strongly photodegraded diatom cells from
600 the Antarctic under darkness in the presence of Fe²⁺ ions showed that HBI trienes **22** and **23**
601 are autoxidized at a similar rate to PUFAs and faster than the chlorophyll phytyl side-chain
602 (**1**), MUFAs and sterols in diatom cells (Rontani et al., 2014a).

603 Autoxidation of IP₂₅ (**19**) involves hydrogen atom abstraction by peroxy radicals at the
604 allylic carbon C-22 and the tertiary carbon atoms C-2, C-6, C-10 and C-14 (Rontani et al.,
605 2018) (Fig. 16). Subsequent oxidation of the resulting radicals, together with hydrogen
606 abstraction from other substrate molecules, leads to the formation of various hydroperoxides,
607 which could be quantified following NaBH₄ reduction as the corresponding alcohols **51–55**
608 (Fig. 16). The failure to detect any autoxidation products resulting from reaction with the
609 tertiary carbon C-7 was attributed to steric hindrance during hydrogen abstraction (Rontani et
610 al., 2018). Compounds **51–55** have thus been proposed as potential tracers of IP₂₅
611 autoxidation.

612 It is well-known that addition of ROO• radicals to a C=C bond competes with allylic
613 hydrogen abstraction when there is a double bond that is either conjugated, tri-substituted or
614 1,1-disubstituted (Schaich, 2005). Consistent with this, efficient addition of peroxy radicals
615 to the 1,1-disubstituted 6-17 double bond of IPSO₂₅ (**20**) was observed (Rontani et al.,
616 2019b); this addition affording the epoxide **56** after fast intramolecular homolytic substitution
617 (Fossey et al., 1995) (Fig. 17). In parallel, allylic hydrogen abstraction at carbon atoms C-5
618 and C-22 also occurred, but to a lesser extent, leading to the formation of hydroperoxides,
619 identifiable via their respective alcohols **57** and **58** following NaBH₄ reduction (Fig. 17).
620 Unfortunately, the well-known biotic and abiotic lability of epoxides in sediments and during
621 sample treatment (Marchand and Rontani, 2001) precludes the use of the major oxidation
622 product **56** as a tracer of IPSO₂₅ autoxidation. In contrast, the alcohols **57** and **58** have the
623 potential to fulfil this role.

624 Hydrogen abstraction at the very reactive bis-allylic C-8 position constitutes the major
625 autoxidation pathway of HBI trienes **22** and **23**. However, the two resulting isomeric
626 hydroperoxides contain conjugated diene structures (Fig. 18), which are particularly prone to
627 addition by peroxy radicals and therefore readily undergo copolymerization with oxygen
628 (Yin et al., 2011) affording highly oxidized products that are not amenable to analysis using
629 gas chromatography (Rontani et al., 2014a). Addition of ROO• radicals to the C9-10 and C7-
630 20 double bonds also takes place as a minor pathway yielding epoxides **59** and **60**,
631 respectively (Fig. 18), and isomeric hydroperoxides (quantifiable under the form of the
632 alcohols **40–42** and **61**) after reaction with oxygen and elimination of a hydroperoxyl radical
633 (Rontani et al., 2014a). It may be noted that the formation of compounds **41** and **42** can also
634 result from hydrogen atom abstraction from the allylic position (C-11) of the parent HBI and
635 subsequent oxidation of the radicals thus formed (Fig. 18). Compounds **40–42** and **61** were
636 not accumulated during the incubations, probably due to their further oxidation to polar and

637 oligomeric compounds, which are not detectable using conventional GC–MS methods.
638 Although alcohols **40–42** may also be produced by Type II photosensitized oxidation (Fig. 8),
639 compound **61** could be identified as a specific (but only qualitative) tracer for autoxidation of
640 HBI trienes **22** and **23** (Rontani et al., 2014a).

641 On the basis of their very weak autoxidation rates (Table 5), it was initially considered
642 that IP₂₅ (**19**) and IPSO₂₅ (**20**) should be unaffected by autoxidation processes within the
643 water column (Rontani et al., 2014a), and the failure to detect autoxidation products **51–55**
644 (Fig. 16) and **57** and **58** (Fig. 17) in suspended particulate matter collected from the Arctic
645 and Antarctic (Rontani et al., 2018, 2019a) certainly supports this assumption. In contrast,
646 these same autoxidation products could be detected in surficial sediments collected from the
647 same regions, albeit in relatively small amounts (Rontani et al., 2018, 2019b). The
648 susceptibility of IP₂₅ (**19**) and IPSO₂₅ (**20**) towards autoxidation thus appears to be most
649 prevalent in cases where sequestered algal material experiences long residence times in the
650 oxic layer of sediments.

651 In contrast to IP₂₅ and IPSO₂₅, the very reactive bis-allylic C-8 position in HBI trienes
652 **22** and **23** should make these HBIs much more sensitive to autoxidation in the marine
653 environment. In support of this, alcohol **61** (Fig. 18) could be detected in Arctic sea ice
654 (Rontani et al., 2014b) and in weakly oxidized samples of phytoplanktonic cells collected
655 from Commonwealth Bay (East Antarctica) (Rontani et al., 2019a), providing direct evidence
656 for the involvement of autoxidation of these HBIs in these regions. However, the lability of
657 this tracer prevented quantitative estimates of autoxidation.

658

659 *4.3.6. Vitamin E*

660 Vitamin E reacts rapidly with peroxy radicals, producing small amounts of 4,7,12-
661 trimethyltridecanoic acid (**15**), 6,10,14-trimethylpentadecan-2-one (**16**), 4,8,12,16-

662 tetramethylheptadecan-4-olide (**17**), α -tocopherylquinone (**18**), and various dimers and
663 trimers as major oxidation products (Liebler, 1994; Frankel, 1998; Rontani et al., 2007b) (Fig.
664 9). However, as described previously (see Section 3.1.4.8), autoxidation products of vitamin E
665 cannot be differentiated from those arising from photooxidation.

666

667 **5. Summary**

668 To be most useful as indicators of lipid oxidation processes, the products of these
669 reactions need to be sufficiently specific to each lipid class and degradation route, and of
670 sufficient stability to enable their identification and quantification. Ideally, their quantification
671 should also provide further information about the extent of the associated degradation process.
672 Thus, they should be sufficiently accumulated and unaffected by secondary oxidation (or
673 other) reactions that would otherwise lead to underestimates or the formation of oligomeric
674 oxidation products that are generally challenging to identify using conventional analytical
675 methods such as GC–MS. This is less of a problem, however, if the primary oxidation
676 products are recalcitrant towards degradation or are degraded (biotically and abiotically) at
677 similar rates compared to their parent compounds. According to their specificity, such lipid
678 oxidation compounds therefore have the potential to provide either qualitative or semi-
679 quantitative information about photooxidation, autoxidation or the total abiotic degradation
680 state of individual or groups of organisms.

681 According to current knowledge, the lipid oxidation products of MUFAs, the phytol
682 side-chain of chlorophyll and Δ^5 -sterols all appear to be widespread in the marine
683 environment (Table 1) and fulfil some of these criteria. Although MUFA oxidation products
684 have proven to be sensitive markers allowing changes in degradation to be monitored as the
685 algal blooms evolved (Christodoulou et al., 2009), a better and more sensitive monitoring of
686 algal stress could be carried out with PUFA oxidation products. The characterisation and

687 quantification of such structures in natural samples constitutes an exciting challenge for the
688 future. In the case of chlorophyll, CPPI is commonly used to estimate the photodegradation
689 percentage in natural marine samples according to the empirical relationship developed by
690 Cuny et al. (2002) (Eqn. 1). Finally, for sterols, the stability and specific nature of the
691 products resulting from individual degradation routes has enabled the relative effects of
692 photo- and autoxidation degradation processes on specific phyla of phytoplankton (e.g.,
693 diatoms, haptophytes, chlorophytes) (Rontani et al., 2012, 2019a), seagrasses (Rontani et al.,
694 2014c; Rontani, 2019) and terrestrial higher plants (Rontani et al., 2014d; Rontani, 2019) to
695 be elucidated.

696 In contrast, the primary degradation products of alkenone (autoxidation) and HBIs
697 (photo- and autoxidation), although useful from a qualitative perspective, appear to be too
698 unstable with respect to secondary oxidation or other reactions for quantification of such
699 pathways. However, the co-measurement of the autoxidation products of the phytyl side-chain
700 of chlorophyll and Δ^5 -sterols has been used to provide indirect evidence for significant
701 alkenone autoxidation, which would result in an overestimation of $U_{37}^{K'}$ values (Christodoulou
702 et al., 2009; Rontani et al. 2009). Similarly, the quantification of autoxidation products of Δ^5 -
703 sterols and palmitoleic acid was recently employed to provide indirect evidence for the
704 influence of autoxidative processes upon the tri-unsaturated HBI triene **22** in phytoplankton
705 samples from the Antarctic (Rontani et al., 2019a). More generally, however, the impact of
706 abiotic degradation on alkenones and HBIs on their use as proxies for palaeo SST and sea ice
707 reconstructions, respectively, remains largely unknown and is in need of further investigation.

708

709 **Acknowledgements**

710 Financial support over many years from the Centre National de la Recherche
711 Scientifique (CNRS), the Aix-Marseille University, and the University of Plymouth is

712 gratefully acknowledged. Thanks are due to the FEDER OCEANOMED (N° 1166-39417) for
713 funding some of the apparatus employed. We are grateful to Dr. Marcel van der Meer and an
714 anonymous reviewer for their useful and constructive comments.

715

716 *Associate Editor*–**Marcus Elvert**

717

718 **References**

- 719 Afi, L., Metzger, P., Largeau, C., Connan, J., Berkaloff, C., Rousseau, B., 1996. Bacterial
720 degradation of green macroalgae: incubation of *Chlorella emersonii* and *Chlorella*
721 *vulgaris* with *Pseudomonas oleovorans* and *Flavobacterium aquatile*. *Organic*
722 *Geochemistry* 25, 117–130.
- 723 Amiraux, R., Jeanthon, C., Vaultier, F., Rontani, J.-F., 2016. Paradoxical effects of
724 temperature and solar irradiance on the photodegradation state of killed
725 phytoplankton. *Journal of Phycology* 52, 475–485.
- 726 Bale, N.J., Airs, R.L., Kimmance, S.A., Llewellyn, C.A., 2013. Transformation of chlorophyll
727 a during viral infection of *Emiliania huxleyi*. *Aquatic Microbial Ecology* 69, 205–210.
- 728 Belicka, L.L., MacDonald, R.W., Harvey, H.R., 2002. Sources and transport of organic
729 carbon to shelf, slope, and basin surface sediments of the Arctic Ocean. *Deep-Sea*
730 *Research I* 49, 1463–1483.
- 731 Belt, S.T., 2018. Source-specific biomarkers as proxies for Arctic and Antarctic sea ice.
732 *Organic Geochemistry* 125, 273–295.
- 733 Belt, S.T., Cooke, D.A., Robert, J.-M., Rowland, S.J., 1996. Structural characterisation of
734 widespread polyunsaturated isoprenoid biomarkers: A C₂₅ triene, tetraene and pentaene
735 from the diatom *Haslea ostrearia* Simonsen. *Tetrahedron Letters* 37, 4755–4758.

- 736 Belt, S.T., Allard, W.G., Massé, G., Robert, J.-M., Rowland, S.J., 2000. Highly branched
737 isoprenoids (HBIs): identification of the most common and abundant sedimentary
738 isomers. *Geochimica et Cosmochimica Acta* 64, 3839–3851.
- 739 Belt, S.T., Massé, G., Allard, W.G., Robert, J.-M., Rowland, S.J., 2001. C₂₅ highly branched
740 isoprenoid alkenes in planktonic diatoms of the *Pleurosigma* genus. *Organic*
741 *Geochemistry* 32, 1271–1275.
- 742 Belt, S.T., Massé, G., Rowland, S.J., Poulin, M., Michel, C., LeBlanc, B., 2007. A novel
743 chemical fossil of palaeo sea ice: IP₂₅. *Organic Geochemistry* 38, 16–27.
- 744 Belt, S.T., Cabedo-Sanz, P., Smik, L., Navarro-Rodriguez, A., Berben, S.M. P., Knies, J.,
745 Husum, K., 2015. Identification of paleo Arctic winter sea ice limits and the marginal
746 ice zone: optimised biomarker-based reconstructions of late Quaternary Arctic sea ice.
747 *Earth and Planetary Science Letters* 431, 127–139.
- 748 Belt, S.T., Smik, L., Brown, T.A., Kim, J.H., Rowland, S.J., Allen, C.S., Gal, J.K., Shin,
749 K.H., Lee, J.I., Taylor, K.W.R., 2016. Source identification and distribution reveals
750 the potential of the geochemical Antarctic sea ice proxy IPSO₂₅. *Nature*
751 *Communications* 7, 12655.
- 752 Belt, S.T., Brown, T.A., Smik, L., Tatarek, A., Wiktor, J., Stowasser, G., Assmy, P., Allen,
753 C.S., Husum, K., 2017. Identification of C₂₅ highly branched isoprenoid (HBI) alkenes
754 in diatoms of the genus *Rhizosolenia* in polar and sub-polar marine phytoplankton.
755 *Organic Geochemistry* 110, 65–72.
- 756 Belt, S.T., Smik, L., Köseoğlu, D., Knies, K., Husum, K., 2019. A novel biomarker-based
757 proxy for the spring phytoplankton bloom in Arctic and sub-arctic settings – HBI T₂₅.
758 *Earth and Planetary Science Letters* 523, 115703.
- 759 Berkessel, A., 2014. *Science of Synthesis: Houben-Weyl Methods of Molecular*
760 *Transformations*, Vol. 38: Peroxides. Georg Thieme Verlag, p. 75.

- 761 Beutner, S., Bloedorn, B., Hoffman, T., Martin, H.D., 2000. Synthetic singlet oxygen
762 quenchers. In: Packer, L., Sies, H. (Eds.), *Methods in Enzymology*, vol. 319.
763 Academic Press, New York, pp. 226–241.
- 764 Bianchi, T.S., Canuel, E.A., 2011. *Chemical Biomarkers in Aquatic Ecosystems*. Princeton
765 University Press, Princeton and Oxford.
- 766 Bidle, K.D., Falkowski, P.G., 2004. Cell death in planktonic, photosynthetic microorganisms.
767 *Nature Review* 2, 643–655.
- 768 Boon, J.J., van der Meer, F.W., Schuyl, P.J., de Leeuw, J.W., Schenck, P.A., Burlingame,
769 A.L., 1978. Organic geochemical analyses of core samples from site 362 Walvis
770 Ridge. DSDP Leg 40, Initial Reports. DSDP Leg 38, 39, 40 and 41, Supplement, pp.
771 627–637.
- 772 Brassell, S.C., 1993. Applications of biomarkers for delineating marine paleoclimatic
773 fluctuations during the Pleistocene. In: Engel, M.H., Macko, S.A. (Eds.), *Organic*
774 *Geochemistry: Principles and Applications*. Plenum Press, New York, pp. 699–738.
- 775 Brassell, S.C., Eglinton, G., Marlowe, I.T., Pflaumann, U., Sarnthein, M., 1986. Molecular
776 stratigraphy: a new tool for climatic assessment. *Nature* 320, 129–133.
- 777 Brown, M.R., Mular, M., Miller, I., Farmer, C., Trenerry, C., 1999. The vitamin content of
778 microalgae used in aquaculture. *Journal of Applied Phycology* 11, 247–255.
- 779 Brown, T.A., Belt, S.T., 2016. Novel tri- and tetra-unsaturated highly branched isoprenoid
780 (HBI) alkenes from the marine diatom *Pleurosigma intermedium*. *Organic*
781 *Geochemistry* 91, 120–122.
- 782 Brown, T.A., Belt, S.T., Cabedo-Sanz, P., 2014. Identification of a novel di-unsaturated C₂₅
783 highly branched isoprenoid lipid in the marine tube-dwelling diatom *Berkeleya*
784 *rutilans*. *Environmental Chemistry Letters*. 12, 455–460.

- 785 Christodoulou, S., Marty, J.-C., Miquel, J.-C., Volkman, J.K., Rontani, J.-F., 2009. Use of
786 lipids and their degradation products as biomarkers for carbon cycling in the
787 northwestern Mediterranean Sea. *Marine Chemistry* 113, 25–40.
- 788 Christodoulou, S., Joux, F., Marty, J.-C., Sempéré, R., Rontani, J.-F., 2010. Comparative
789 study of UV and visible light induced degradation of lipids in non-axenic senescent
790 cells of *Emiliania huxleyi*. *Marine Chemistry* 119, 139–152.
- 791 Clough, R.L., Yee, B.G., Foote, C.S., 1979. Chemistry of singlet oxygen. The unstable
792 primary product of tocopherol photooxidation. *Journal of the American Chemical*
793 *Society* 101, 683–686.
- 794 Cuny, P., Rontani, J.-F., 1999. On the widespread occurrence of 3-methylidene-7,11,15-
795 trimethylhexadecan-1,2-diol in the marine environment: a specific isoprenoid marker
796 of chlorophyll photodegradation. *Marine Chemistry* 65, 155–165.
- 797 Cuny, P., Romano, J.-C., Beker, B., Rontani, J.-F., 1999. Comparison of the photo-
798 degradation rates of chlorophyll chlorin ring and phytol side chain in phytodetritus: is
799 the phytyldiol versus phytol ratio (CPPI) a new biogeochemical index? *Journal of*
800 *Experimental Marine Biology and Ecology* 237, 271–290.
- 801 Cuny, P., Marty, J.-C., Chiaverini, J., Vescovali, I., Raphel, D., Rontani, J.-F., 2002. One-year
802 seasonal survey of the chlorophyll photodegradation process in the Northwestern
803 Mediterranean Sea. *Deep-Sea Research II* 49, 1987–2005.
- 804 Devasagayam, T., Kamat, J., 2002. Biological significance of singlet oxygen. *Indian Journal*
805 *of Experimental Biology* 40, 680–692.
- 806 de Leeuw, J.W., van der Meer, J.W., Rijpstra, W.I.C., Schenck, P.A., 1980. On the occurrence
807 and structural identification of long chain ketones and hydrocarbons in sediments. In:
808 Douglas, A.G., Maxwell, J.R. (Eds.), *Advances in Organic Geochemistry 1979*.
809 Pergamon Press, Oxford, pp. 211–217.

- 810 Eltgroth, M.L., Watwood, R.L., Wolfe, G.V., 2005. Production and cellular localization of
811 neutral long-chain lipids in the Haptophyte algae *Isochrysis galbana* and *Emiliania*
812 *huxleyi*. *Journal of Phycology* 41, 1000–1009.
- 813 Engel, N., Jenny, T.A., Mooser, V., Gossauer, A., 1991. Chlorophyll catabolism in *Chlorella*
814 *protothecoides*. Isolation and structure elucidation of a red bilin derivative. *FEBS*
815 *Letters* 293, 131–133.
- 816 Ehrenberg, B., Anderson, J.L., Foote, C.S., 1998. Kinetics and yield of singlet oxygen
817 photosensitized by hypericin in organic and biological media. *Photochemistry and*
818 *Photobiology* 68, 135–140.
- 819 Fischer, B.B., Krieger-Liszkay, A., Hideg, E., Šnyrychová, I., Wiesendanger, M., Eggen,
820 R.I.L., 2007. Role of singlet oxygen in chloroplast to nucleus retrograde signaling in
821 *Chlamydomonas reinhardtii*. *FEBS Letters* 581, 5555–5560.
- 822 Foote, C.S., 1976. Photosensitized oxidation and singlet oxygen: consequences in biological
823 systems. In: Pryor, W.A. (Ed.), *Free Radicals in Biology*. Academic Press, New York,
824 pp. 85–133.
- 825 Fossey, J., Lefort, D., Sorba, J., 1995. *Free Radicals in Organic Chemistry*. Masson, Paris, pp.
826 1–307.
- 827 Frankel, E.N., 1998. *Lipid Oxidation*. The Oily Press, Dundee.
- 828 Frankel, E.N., Neff, W.E., Bessler, T.R., 1979. Analysis of autoxidized fats by gas
829 chromatography-mass spectrometry: V. photosensitized oxidation. *Lipids* 14, 961–
830 967.
- 831 Franklin, D.J., Airs, R.L., Fernandes, M., Bell, T.G., Bongaerts, R.J., Berges, J.A., Malin, G.,
832 2012. Identification of senescence and death in *Emiliania huxleyi* and *Thalassiosira*
833 *pseudonana*: cell staining, chlorophyll alterations, and dimethylsulfoniopropionate
834 (DMSP) metabolism. *Limnology and Oceanography* 57, 305–317.

- 835 Frimer, A.A., 1979. The reaction of singlet oxygen with olefins: the question of mechanism.
836 *Chemical Review* 79, 359–387.
- 837 Frimer, A.A., 1983. Singlet oxygen in peroxide chemistry. In: Patai, S. (Ed.), *The Chemistry*
838 *of Functional Groups, Peroxides*. John Wiley & Sons Ltd., pp. 202–229.
- 839 Fuchs, C., Spitteller, G., 2014. Iron release from the active site of lipoxygenase. *Zeitschrift für*
840 *Naturforschung C* 55, 643–648.
- 841 Galeron, M.-A., Amiraux, R., Charriere, B., Radakovitch, O., Raimbault, P., Garcia, N.,
842 Lagadec, V., Vaultier, F., Rontani J.-F., 2015. Source and behavior of particulate
843 organic matter in the Rhône River: a lipid approach. *Biogeosciences*. 12, 1431–1446.
- 844 Galeron, M.-A., Radakovitch, O., Charriere, B., Vaultier, F., Volkman, J.K., Bianchi, T.S.,
845 Ward, N.T., Medeiros, P., Sawakuchi, H., Tank, S., Kerhervé, P., Rontani, J-F., 2018.
846 Lipoxygenase-induced autoxidative degradation of terrestrial particulate organic
847 matter in estuaries: a widespread process enhanced at high and low latitudes. *Organic*
848 *Geochemistry* 115, 78–92.
- 849 Gelin, F., Boogers, I., Noordeloos, A.A.M., Sinninghe Damsté, J.S., Riegman, R., de Leeuw,
850 J.W., 1997. Resistant biomacromolecules in marine microalgae of the classes
851 Eustigmatophyceae and Chlorophyceae: Geochemical implications. *Organic*
852 *Geochemistry* 26, 659–675.
- 853 Girotti, A.W., 1998. Lipid hydroperoxide generation, turnover, and effector action in
854 biological systems. *Journal of Lipid Research* 39, 1529–1542.
- 855 Goad, L.J., 1981. Sterol biosynthesis and metabolism in marine invertebrates. *Pure and*
856 *Applied Chemistry* 53, 837–852.
- 857 Gollnick, K., 1968. Type II Photooxygenation Reactions in Solution. In: Noyes, W.A.,
858 Hammond, G.S., Pitts, J.N. (Eds.), *Advances in Photochemistry* vol. 6. Wiley.

- 859 Griesbeck, A.G., Adam, W., Bartoscheck, A., El-Idreesy, T.T., 2003. Photooxygenation of
860 allylic alcohols: kinetic comparison of unfunctionalized alkenes with prenyl-type
861 allylic alcohols, ethers and acetates. *Photochemistry and Photobiology Sciences* 2,
862 877–881.
- 863 Halliwell, B., 1987. Oxidative damage, lipid peroxidation and antioxidant protection in
864 chloroplasts. *Chemistry and Physics of lipids* 44, 327–340.
- 865 Harnett, H.E., Keil, R.G., Hedges, J.I., Devol, A.H., 1998. Influence of oxygen exposure time
866 on organic matter preservation in continental margin sediments. *Nature* 391, 572–574.
- 867 Heath, R.L., Packer, L., 1968. Photoperoxidation in isolated chloroplasts. II. Role of electron
868 transfer. *Archives of Biochemistry and Biophysics* 125, 850–857.
- 869 Henrich, R., 1991. Cycles, rhythms, and events on high input and low input glaciated
870 continental margins. In: Einsele, G., Ricken, W., Seilacher, A. (Eds.), *Cycles and*
871 *Events in Stratigraphy*. Springer, Berlin Heidelberg, pp. 751–772.
- 872 Huang, J.J., Lin, S., Xu, W., Cheung, P.C.K., 2017. Occurrence and biosynthesis of
873 carotenoids in phytoplankton. *Biotechnology Advances* 35, 597–618.
- 874 Hurst, J.R., Wilson, S.L., Schuster, G.B., 1985. The ene reaction of singlet oxygen: kinetic
875 and product evidence in support of a perepoxide intermediate. *Tetrahedron* 41, 2191–
876 2197.
- 877 Hynninen, P.H., 1991. Chemistry of chlorophylls: modifications. In: Scheer, H. (Ed.),
878 *Chlorophylls*. CRC Press, London, pp. 145–209.
- 879 Ingold, K.U., 1969. Peroxy radicals. *Accounts for Chemical Research* 2, 1–9.
- 880 Iseo, S., Hyeon, S.B., Katsumura, S., Sakan, T., 1972. Photooxygenation of carotenoids. II–
881 The absolute configuration of loliolide and dihydroactinidiolide. *Tetrahedron Letters*
882 25, 2517–2520.

- 883 Iturraspe, J., Engel, N., Gossauer, A., 1994. Chlorophyll catabolism. Isolation and structure
884 elucidation of chlorophyll b catabolites in *Chlorella protothecoides*. *Phytochemistry*
885 35, 1387–1390.
- 886 Jaraula, C.M.B., Brassell, S.C, Morgan-Kiss, R, Doran, P.T., Kenig, F., 2010. Origin and
887 distribution of tri to pentaunsaturated alkenones in Lake Fryxell, East Antarctica.
888 *Organic Geochemistry* 41, 386–397.
- 889 Jeffrey, S.W., Hallegraeff, G.M., 1987. Chlorophyllase distribution in ten classes of
890 phytoplankton: a problem for chlorophyll analysis. *Marine Ecology Progress Series*
891 35, 293–304.
- 892 Jónasdóttir, S.H., 2019. Fatty acid profiles and production in marine phytoplankton. *Marine*
893 *Drugs* 17, 151. <https://doi.org/10.3390/md17030151>.
- 894 Kaiser, J., Belt, S.T., Tomczak, T., Brown, T.A., Wasmund, N., Arz, H.W., 2016. C₂₅ highly
895 branched isoprenoid alkenes in the Baltic Sea produced by the marine planktonic
896 diatom *Pseudosolenia calcar-avis*. *Organic Geochemistry* 93, 51–58.
- 897 Knox, J.P., Dodge, A.D., 1985. Singlet oxygen and plants. *Phytochemistry* 24, 889–896.
- 898 Kopecky, K.R., Reich, H.J., 1965. Reactivities in photosensitized olefin oxidations. *Canadian*
899 *Journal of Chemistry* 43, 2265–2270.
- 900 Korytowski, W., Bachowski, G.J., Girotti, A.W., 1992. Photoperoxidation of cholesterol in
901 homogeneous solution, isolated membranes, and cells: comparison of the 5 α - and 6 β -
902 hydroperoxides as indicators of singlet oxygen intermediacy. *Photochemistry and*
903 *Photobiology* 56, 1–8.
- 904 Köseoğlu, D., Belt, S.T., Smik, L., Yao, H., Panieri, G., Knies, J., 2018. Complementary
905 biomarker-based methods for characterising Arctic sea ice conditions: A case study
906 comparison between multivariate analysis and the PIP₂₅ index. *Geochimica et*
907 *Cosmochimica Acta* 222, 406–420.

- 908 Köseoğlu, D., Belt, S.T., Husum, K., Knies, J., 2018. An assessment of biomarker-based
909 multivariate classification methods versus the PIP₂₅ index for paleo Arctic sea ice
910 reconstruction. *Organic Geochemistry* 125, 82–94.
- 911 Krasnovsky Jr, A.A., 1998. Singlet molecular oxygen in photobiochemical systems: IR
912 phosphorescence studies. *Membrane Cellular Biology* 12, 665–690.
- 913 Kulig, M.J., Smith, L.L., 1973. Sterol metabolism. XXV. Cholesterol oxidation by singlet
914 molecular oxygen. *Journal of Organic Chemistry* 38, 3639–3642.
- 915 Leshem, Y.Y., 1988. Plant senescence processes and free radicals. *Free Radical in Biology*
916 *and Medicine* 5, 39–49.
- 917 Liebler, D.C., 1994. Tocopherone and epoxytocopherone products of vitamin E oxidation.
918 *Methods in Enzymology* 234, 310–316.
- 919 Mäkinen, K., Elfving, M., Hänninen, J., Laaksonen, L., Rajasilta, M., Vuorinen, I., Suomela,
920 J.-P., 2017. Fatty acid composition and lipid content in the copepod *Limnocalanus*
921 *macrurus* during summer in the southern Bothnian Sea. *Helgoland Marine Research*
922 71:11. DOI 10.1186/s10152-017-0491-1
- 923 Marchand, D., Rontani, J.-F., 2001. Characterisation of photooxidation and autoxidation
924 products of phytoplanktonic monounsaturated fatty acids in marine particulate matter
925 and recent sediments. *Organic Geochemistry* 32, 287–304.
- 926 Marchand, D., Marty, J.-C., Miquel, J.-C., Rontani, J.-F., 2005. Lipids and their oxidation
927 products as biomarkers for carbon cycling in the northwestern Mediterranean Sea:
928 results from a sediment trap study. *Marine Chemistry* 95, 129–147.
- 929 Marlowe, I.T., Green, J.C., Neal, A.C., Brassell, S.C., Eglinton, G., Course, P.A., 1984. Long
930 chain (*n*-C₃₇–C₃₉) alkenones in the Prymnesiophyceae. Distribution of alkenones and
931 other lipids and their taxonomic significance. *British Phycology Journal* 19, 203–216.

- 932 Mayer, L.M., Schick, L.L., Hardy, R., Estapa, M.L., 2009. Photodissolution and other
933 photochemical changes upon irradiation of algal detritus. *Limnology and*
934 *Oceanography* 54, 1688–1698.
- 935 Merzlyak, M.N., Hendry, G.A.F., 1994. Free radical metabolism, pigment degradation and
936 lipid peroxidation in leaves during senescence. *Proceedings of the Royal Society of*
937 *Edinburgh* 102B, 459–471.
- 938 Morley, C.P., Mainwaring, K.A., Doerr, S.H., Douglas, P., Llewellyn, C.T., Dekker, L.W.,
939 2005. Organic compounds at different depths in a sandy soil and their role in water
940 repellency. *Australian Journal of Soil Research* 43, 239–249.
- 941 Morrissey, P.A., Kiely, M., 2006. Oxysterols: formation and biological function. In: Fox,
942 P.F., McSweeney, P.L.H. (Eds.), *Advanced Dairy Chemistry* 3rd edition, Vol. 2,
943 *Lipids*, Springer, New York, pp. 641–674.
- 944 Mouzdahir A., Grossi, V., Bakkas, S., Rontani, J.-F., 2001. Photodegradation of long-chain
945 alkenes in senescent cells of *Emiliania huxleyi* and *Nannochloropsis salina*.
946 *Phytochemistry* 56, 677–684.
- 947 Müller, P.J., Kirst, G., Ruhland, G., von Storch, I., Rosell-Melé, A., 1998. Calibration of the
948 alkenone paleotemperature index $U_{37}^{K'}$ based on core-tops from the eastern South
949 Atlantic and global ocean (60°N–60°S). *Geochimica et Cosmochimica Acta* 62, 1757–
950 1772.
- 951 Nassiry, M., Aubert, C., Mouzdahir, A., Rontani, J.-F., 2009. Generation of isoprenoid
952 compounds and notably of prist-1-ene through photo- and autoxidative degradation of
953 vitamin E. *Organic Geochemistry* 40, 38–50.
- 954 Neff, W.E., Frankel, E.N., Fujimoto, K., 1988. Autoxidative dimerization of methyl linolenate
955 and its monohydroperoxides, hydroperoxy epidioxides and dihydroperoxides. *Journal*
956 *of the American Oil Chemical Society* 65, 616–623.

- 957 Nelson, J.R., 1993. Rates and possible mechanism of light-dependent degradation of pigments
958 in detritus derived from phytoplankton. *Journal of Marine Research* 51, 155–179.
- 959 Nickon, A., Bagli, J.F., 1961. Reactivity and geochemistry in allylic systems. I.
960 Stereochemistry of photosensitized oxygenation of monoolefins. *Journal of the*
961 *American Chemical Society* 83, 1498–1508.
- 962 Orfanopoulos, M., Stratakis, M., Elemen, Y., 1989. Regioselective reaction of singlet oxygen
963 with *cis*-alkenes. *Tetrahedron Letters* 30, 4871–4874.
- 964 Piepho, M., Martin-Creuzburg, D., Wacker, A., 2012. Phytoplankton sterol contents vary with
965 temperature, phosphorus and silicate supply: a study on three freshwater species.
966 *European Journal of Phycology* 47, 138–145.
- 967 Pokorny, J., 1987. Major factors affecting the autoxidation of lipids. In: Chan, H.W.-S. (Ed.),
968 *Autoxidation of Unsaturated Lipids*. Academic Press, London, pp. 141–206.
- 969 Porter, N.A., Caldwell, S.E., Mills, K.A., 1995. Mechanisms of free radical oxidation of
970 unsaturated lipids. *Lipids* 30, 277–290.
- 971 Prah, F.G., Wakeham, S.G., 1987. Calibration of unsaturation patterns in long-chain ketone
972 compositions for palaeotemperature assessment. *Nature* 330, 367–369.
- 973 Prah, F.G., Muehlhausen, L.A., Zahnle, D.L., 1988. Further evaluation of long-chain
974 alkenones as indicators of paleoceanographic conditions. *Geochimica et*
975 *Cosmochimica Acta* 52, 2303–2310.
- 976 Prah, F.G., Rontani, J.-F., Volkman, J.K., Sparrow, M.A., Royer, I.M., 2006. Unusual C₃₅
977 and C₃₆ alkenones in a paleoceanographic benchmark strain of *Emiliana huxleyi*.
978 *Geochimica et Cosmochimica Acta* 70, 2856–2867.
- 979 Rechka, J.A., Maxwell, J.R., 1988. Unusual long chain ketones of algal origin. *Tetrahedron*
980 *Letters* 29, 2599–2600.

- 981 Repeta, D.J., 1989. Carotenoid diagenesis in recent marine sediments. II– Degradation of
982 fucoxanthin to loliolide. *Geochimica et Cosmochimica Acta* 53, 699–707.
- 983 Rieley, G., Teece, M. A., Peakman, T. M., Raven, A. M., Greene, K. J., Clarke, T. P., Murray,
984 M., Leftley, J. W., Campbell, C. N., Harris, R. P., Parkes, R. J., Maxwell, J. R., 1998.
985 Long-chain alkenes of the Haptophytes *Isochrysis galbana* and *Emiliania huxleyi*.
986 *Lipids* 33, 617–625.
- 987 Rontani, J.-F., 2012. Photo- and free radical-mediated oxidation of lipid components during
988 the senescence of phototrophic organisms. In: Nagata, T. (Ed.), *Senescence*, Intech,
989 Rijeka, pp. 3–31.
- 990 Rontani, J.-F., 2019. Biotic and abiotic degradation of Δ^5 -sterols in senescent Mediterranean
991 marine and terrestrial angiosperms. *Phytochemistry* 167
992 doi.org/10.1016/j.phytochem.2019.112097.
- 993 Rontani, J.-F., Aubert, C., 1994. Effect of oxy-free radicals upon the phytyl chain during
994 chlorophyll-a photodegradation. *Journal of Photochemistry and Photobiology A79*,
995 167–172.
- 996 Rontani, J.-F., Aubert, C., 2005. Characterization of isomeric allylic diols resulting from
997 chlorophyll phytyl side chain photo- and autoxidation by electron ionization gas
998 chromatography/mass spectrometry. *Rapid Communications in Mass Spectrometry* 19,
999 637–646.
- 1000 Rontani, J.-F., Volkman, J.K., 2005. Lipid characterisation of coastal hypersaline
1001 cyanobacterial mats from the Camargue (France). *Organic Geochemistry* 36, 251–272.
- 1002 Rontani, J.-F., Galeron, M.-A., 2016. Autoxidation of chlorophyll phytyl side-chain in
1003 senescent phototrophic organisms: a potential source of isophytol in the environment.
1004 *Organic Geochemistry* 97, 37–40.

- 1005 Rontani, J.-F., Grossi, V., Faure, F., Aubert, C., 1994. “Bound” 3-methylidene-7,11,15-
1006 trimethylhexadecan-1,2-diol: a new isoprenoid marker for the photodegradation of
1007 chlorophyll-a in seawater. *Organic Geochemistry* 21, 135–142.
- 1008 Rontani, J.-F., Beker, B., Raphel, D., Baillet, G., 1995. Photodegradation of chlorophyll
1009 phytyl chain in dead phytoplanktonic cells. *Journal of Photochemistry and*
1010 *Photobiology* 85A, 137–142.
- 1011 Rontani, J.-F., Cuny, P., Grossi, V., 1996. Photodegradation of chlorophyll phytyl chain in
1012 senescent leaves of higher plants. *Phytochemistry* 42, 347–351.
- 1013 Rontani, J.-F., Cuny, P., Aubert, C., 1997a. Rates and mechanism of light-dependent
1014 degradation of sterols in senescing cells of phytoplankton. *Journal of Photochemistry*
1015 *and Photobiology* 111A, 139–144.
- 1016 Rontani, J.-F., Cuny, P., Grossi, V., Beker, B., 1997b. Stability of long-chain alkenones in
1017 senescing cells of *Emiliana huxleyi*: effect of photochemical and aerobic microbial
1018 degradation on the alkenone unsaturation ratio ($U_{37}^{K'}$). *Organic Geochemistry* 26, 503–
1019 509.
- 1020 Rontani, J.-F., Cuny, P., Grossi, V., 1998. Identification of a pool of lipid photoproducts in
1021 senescent phytoplanktonic cells. *Organic Geochemistry* 29, 1215–1225.
- 1022 Rontani, J.-F., Rabourdin, A., Marchand, D., Aubert, C., 2003. Photochemical oxidation and
1023 autoxidation of chlorophyll phytyl side chain in senescent phytoplanktonic cells:
1024 potential sources of several acyclic isoprenoid compounds in the marine environment.
1025 *Lipids* 38, 241–253.
- 1026 Rontani, J.-F., Marty, J.-C., Miquel, J.-C., Volkman, J.K., 2006. Free radical oxidation
1027 (autoxidation) of alkenones and other microalgal lipids in seawater. *Organic*
1028 *Geochemistry* 37, 354–368.

- 1029 Rontani, J.-F., Jameson, I., Christodoulou, S., Volkman, J.K., 2007a. Free radical oxidation
1030 (autoxidation) of alkenones and other lipids in cells of *Emiliania huxleyi*.
1031 *Phytochemistry* 68, 913–924.
- 1032 Rontani, J.-F., Nassiry, M., Mouzdahir, A., 2007b. Free radical oxidation (autoxidation) of α -
1033 tocopherol (vitamin E): A potential source of 4,8,12,16-tetramethylheptadecan-4-olide
1034 in the environment. *Organic Geochemistry* 38, 37–47.
- 1035 Rontani, J.-F., Harji, R., Volkman, J.K., 2007c. Biomarkers derived from heterolytic and
1036 homolytic cleavage of allylic hydroperoxides resulting from alkenone autoxidation.
1037 *Marine Chemistry* 107, 230–243.
- 1038 Rontani, J.-F., Zabeti, N., Wakeham, S.G., 2009. The fate of marine lipids: Biotic vs. abiotic
1039 degradation of particulate sterols and alkenones in the Northwestern Mediterranean
1040 Sea. *Marine Chemistry* 113, 9–18.
- 1041 Rontani, J.-F., Nassiry, M., Guasco, S., Michotey, V., Bonin P., 2010. Production of pristane
1042 from α -tocopherols under simulated anoxic sedimentary conditions: a combination of
1043 biotic and abiotic degradative processes. *Geochimica et Cosmochimica Acta* 74: 252–
1044 263.
- 1045 Rontani, J.-F., Belt, S.T., Vaultier, F., Brown, T.A., 2011. Visible light-induced photo-
1046 oxidation of highly branched isoprenoid (HBI) alkenes: a significant dependence on
1047 the number and nature of the double bonds. *Organic Geochemistry* 42, 812–822.
- 1048 Rontani, J.-F., Charriere, B., Petit, M., Vaultier, F., Heipieper, H., Link, H., Chailloux, G.,
1049 Sempéré, R., 2012a. Degradation state of organic matter in surface sediments from the
1050 Southern Beaufort Sea: a lipid approach. *Biogeosciences* 9, 3513–3530.
- 1051 Rontani, J.-F., Charriere, B., Petit, M., Vaultier, F., Heipieper, H., Link, H., Chailloux, G.,
1052 Sempéré, R., 2012b. Degradation state of organic matter in surface sediments from the
1053 Southern Beaufort Sea: a lipid approach. *Biogeosciences* 9, 3513–3530.

- 1054 Rontani, J.-F., Volkman, J.K., Prahl, F.G., Wakeham, S.G., 2013. Biotic and abiotic
1055 degradation of alkenones and implications for $U_{37}^{K'}$ paleoproxy applications: A review.
1056 *Organic Geochemistry* 59, 93–113.
- 1057 Rontani, J.-F., Belt, S., Vaultier, F., Brown, T., Massé, G., 2014a. Autoxidative and
1058 photooxidative reactivity of highly branched isoprenoid (HBI) alkenes. *Lipids* 49,
1059 481–494.
- 1060 Rontani, J.-F., Belt, S.T., Brown, T., Vaultier, F., Mundy, C.J., 2014b. Identification of
1061 sequential photo- and autoxidation of diatom lipids in Arctic sea ice. *Organic*
1062 *Geochemistry* 77, 59–71.
- 1063 Rontani, J.-F., Vaultier, F., Bonin, P., 2014c. Biotic and abiotic degradation of marine and
1064 terrestrial higher plant material in intertidal surface sediments from Arcachon Bay
1065 (France): A lipid approach. *Marine Chemistry* 158, 69–79.
- 1066 Rontani, J.-F., Charrière, B., Sempéré, R., Doxaran, D., Vaultier, F., Vonk, J.E., Volkman,
1067 J.K., 2014d. Degradation of sterols and terrigenous organic matter in waters of the
1068 Mackenzie Shelf, Canadian Arctic. *Organic Geochemistry* 75, 61–73.
- 1069 Rontani, J.-F., Belt, S.T., Brown, T.A., Amiriaux, R., Gosselin, M., Vaultier, F., Mundy, C.J.,
1070 2016. Monitoring abiotic degradation in sinking versus suspended Arctic sea ice algae
1071 during a spring ice melt using specific lipid oxidation tracers. *Organic Geochemistry*
1072 98, 82–97.
- 1073 Rontani, J.-F., Galeron, M.-A., Amiriaux, R., Artigue, L., Belt, S.T., 2017. Identification of di-
1074 and triterpenoid lipid tracers confirms the significant role of autoxidation in the
1075 degradation of terrestrial vascular plant material in the Canadian Arctic. *Organic*
1076 *Geochemistry* 108, 43–50.

- 1077 Rontani, J.-F., Belt, S.T., Amiraux, R., 2018. Biotic and abiotic degradation of the sea ice
1078 diatom biomarker IP₂₅ and selected algal sterols in near-surface Arctic sediments.
1079 *Organic Geochemistry* 118, 73–88.
- 1080 Rontani, J.-F., Smik, L., Belt, S.T., Vaultier, F., Armbrecht, L., Leventer, A., Armand, L.K.,
1081 2019a. Abiotic degradation of highly branched isoprenoid alkenes and other lipids in
1082 the water column off East Antarctica. *Marine Chemistry* 210, 34–47.
- 1083 Rontani, J.-F., Smik, L., Belt, S.T., 2019b. Autoxidation of the sea ice biomarker proxy
1084 IPSO₂₅ in the near-surface oxic layers of Arctic and Antarctic sediments. *Organic*
1085 *Geochemistry* 129, 63–76.
- 1086 Rowland, S.J., Robson, J.N., 1990. The widespread occurrence of highly branched isoprenoid
1087 acyclic C₂₀, C₂₅ and C₃₀ hydrocarbons in recent sediments and biota: a review. *Marine*
1088 *Environmental Research* 30, 191–216.
- 1089 Sato, K., Akaike, T., Kohno, M., Ando, M., Maeda, H., 1992. Hydroxyl radical production by
1090 H₂O₂ plus Cu, Zn-superoxide dismutase reflects the activity of free copper released
1091 from the oxidatively damaged enzyme. *Journal of Biological Chemistry* 267, 25371–
1092 25377.
- 1093 Schaich, K.M., 2005. Lipid oxidation: Theoretical aspects. In: Shahidi, F. (Ed.), *Bailey's*
1094 *Industrial Oil and Fat Products*. John Wiley & Sons, Chichester, pp. 269–355.
- 1095 Schwarzbauer, J., Littke, R., Weigelt, V., 2000. Identification of specific organic
1096 contaminants for estimating the contribution of the Elbe River to the pollution of the
1097 German Bight. *Organic Geochemistry* 31, 1713–1731.
- 1098 Sheldon, R.A., Kochi, J.K., 1976. Metal-catalyzed oxidations of organic compounds in the
1099 liquid phase. A mechanistic approach. *Advances in Catalysis* 25, 272–413.
- 1100 Sinninghe Damsté, J.S., Schouten, S., Rijpstra, W.I.C., Hopmans, E.C., Peletier, H., Gieskes,
1101 W.W.C., Geenevasen, J.A.J., 1999. Structural identification of the C₂₅ highly branched

- 1102 isoprenoid pentaene in the marine diatom *Rhizosolenia setigera*. *Organic*
1103 *Geochemistry* 30, 1581–1583.
- 1104 Sinninghe Damsté, J.S., Muyzer, G., Abbas, B., Rampen, S.W., Massé, G., Allard, W.G.,
1105 Belt, S.T., Robert, J.-M., Rowland, S.J., Moldovan, J.M., Barbanti, S.M., Fago, F.J.,
1106 Denisevich, P., Dahl, J., Trindade, L.A.F., Schouten, S., 2004. The rise of the
1107 Rhizosolenid diatoms. *Science* 304, 584–587.
- 1108 Smith, L.L., 1981. *The Autoxidation of Cholesterol*. Plenum Press, New York.
- 1109 Sun, M.-Y., Aller, R.C., Lee, C., Wakeham, S.G., 1999. Enhanced degradation of algal lipids
1110 by benthic macro-faunal activity: effect of *Yoldia limatula*. *Journal of Marine*
1111 *Research* 57, 775–804.
- 1112 Takaichi, S., 2011. Carotenoids in algae: distributions, biosynthesis and functions. *Marine*
1113 *Drugs* 9, 1101–1118.
- 1114 Volkman, J.K. 1986. A review of sterol markers for marine and terrigenous organic matter.
1115 *Organic Geochemistry* 9, 83–99.
- 1116 Volkman, J.K. 2003. Sterols in microorganisms. *Applied Microbiology and Biotechnology*
1117 60, 495–506.
- 1118 Volkman, J.K., Eglinton, G., Corner, E.D.S., Forsberg, T.E.V., 1980. Long chain alkenes and
1119 alkenones in the marine coccolithophorid *Emiliana huxleyi*. *Phytochemistry* 19,
1120 2619–2622.
- 1121 Volkman, J.K., Barrett, S.M., Dunstan, G.A., 1994. C₂₅ and C₃₀ highly branched isoprenoid
1122 alkenes in laboratory cultures of two marine diatoms. *Organic Geochemistry* 21, 407–
1123 414.
- 1124 Volkman, J.K., Barrett, S.M., Blackburn, S.I., Sikes, E.L., 1995. Alkenones in *Gephyrocapsa*
1125 *oceanica* – implications for studies of paleoclimate. *Geochimica et Cosmochimica*
1126 *Acta* 59, 513–520.

- 1127 Volkman, J.K., Barrett, S.M., Blackburn, S.I., Mansour, M.P., Sikes, E.L., Gelin, F., 1998.
1128 Microalgal biomarkers: a review of recent research developments. *Organic*
1129 *Geochemistry* 29, 1163–1179.
- 1130 Wakeham, S.G., Lee, C., Hedges, J.I., Hernes, P.J., Peterson, M.L., 1997. Molecular
1131 indicators of diagenetic status in marine organic matter. *Geochimica et Cosmochimica*
1132 *Acta* 61, 5363–5369.
- 1133 Walker, J.S., Keely, B.J., 2004. Distribution and significance of chlorophyll derivatives and
1134 oxidation products during the spring phytoplankton bloom in the Celtic Sea April
1135 2002. *Organic Geochemistry* 35, 1289–1298.
- 1136 Yamauchi, R., Matsushita, S., 1979. Products formed by photosensitized oxidation of
1137 tocopherols. *Agricultural and Biological Chemistry* 43, 2151–2156.
- 1138 Yin, H., Xu, L., Porter, N.A., 2011. Free radical lipid peroxidation: mechanisms and analysis.
1139 *Chemical Reviews* 111, 5944–5972.
- 1140 Zafiriou, O.C., 1977. Marine organic photochemistry previewed. *Marine Chemistry* 5, 497–
1141 522.
- 1142 Zafiriou, O.C., Jousset-Dubien, J., Zepp, R.G., Zika, R.G., 1984. Photochemistry in natural
1143 waters. *Environmental Science and Technology* 18, 358A–370A.
- 1144 Zolla, L., Rinalducci, S., 2002. Involvement of active oxygen species in degradation of light-
1145 harvesting proteins under light stresses. *Biochemistry* 41, 14391–14402.

1146

1147 **FIGURE CAPTIONS**

1148

1149 **Fig. 1.** Reactions of the excited triplet sensitizer.

1150

1151 **Fig. 2.** Behaviour of the excited singlet state of chlorophyll in healthy (A) and senescent (B)
1152 cells of phytoplankton (simplified schemes taking into account only the involvement of
1153 singlet oxygen).

1154

1155 **Fig. 3.** Type II photosensitized oxidation of the chlorophyll phytyl side-chain (**1**) and
1156 subsequent NaBH₄ reduction and alkaline hydrolysis of the resulting hydroperoxides.

1157

1158 **Fig. 4.** Structures of loliolide (**4**) and *iso*-loliolide (**5**).

1159

1160 **Fig. 5.** Type II photosensitized oxidation of Δ^5 -sterols and subsequent NaBH₄ reduction of the
1161 resulting 6-hydroperoxides.

1162

1163 **Fig. 6.** Type II photosensitized oxidation of MUFAs and subsequent NaBH₄ reduction of the
1164 resulting hydroperoxides.

1165

1166 **Fig. 7.** Structures of HBI alkenes **19–24**.

1167

1168 **Fig. 8.** Type II photosensitized oxidation of HBI trienes **22** and **23** and subsequent NaBH₄
1169 reduction of the resulting hydroperoxides.

1170

1171 **Fig. 9.** Type II photosensitized oxidation and autoxidation of vitamin E (**13**).

1172

1173 **Fig. 10.** Induction of autoxidation processes in senescent phytoplanktonic cells.

1174

1175 **Fig. 11.** Structures of 13²-hydroxychlorophyll a (**43**) and 13²-methoxychlorophyll a (**44**).

1176

1177 **Fig. 12.** Autoxidation of chlorophyll phytyl side-chain (**1**) and subsequent NaBH₄ reduction
1178 and alkaline hydrolysis of the resulting hydroperoxides.

1179

1180 **Fig. 13.** Autoxidation of Δ^5 -sterols and degradation of the oxidation products formed during
1181 the treatment.

1182

1183 **Fig. 14.** Autoxidation of MUFAs and subsequent NaBH₄ reduction of the resulting
1184 hydroperoxides.

1185

1186 **Fig. 15.** Autoxidation of the Δ^8 double bond of C_{37:3} alkenone and subsequent NaBH₄
1187 reduction of the resulting hydroperoxides.

1188

1189 **Fig. 16.** Autoxidation of IP₂₅ (**19**) and subsequent NaBH₄ reduction of the resulting
1190 hydroperoxides.

1191

1192 **Fig. 17.** Autoxidation of IP_{SO₂₅} (**20**) and subsequent NaBH₄ reduction of the resulting
1193 hydroperoxides.

1194

1195 **Fig. 18.** Autoxidation of HBI trienes **22** and **23** and subsequent NaBH₄ reduction of the
1196 resulting hydroperoxides.

1197

1198

Figure 1

“ Disclaimer: This is a pre-publication version. Readers are recommended to consult the full published version for accuracy and citation.”

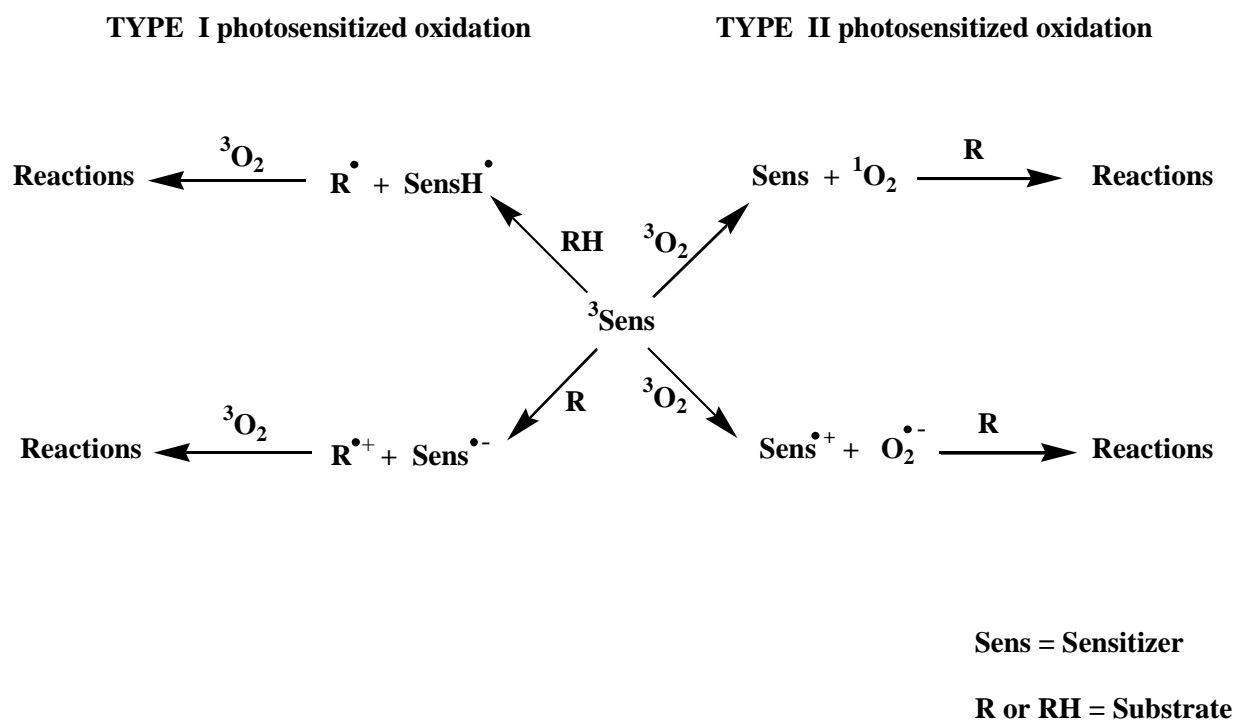
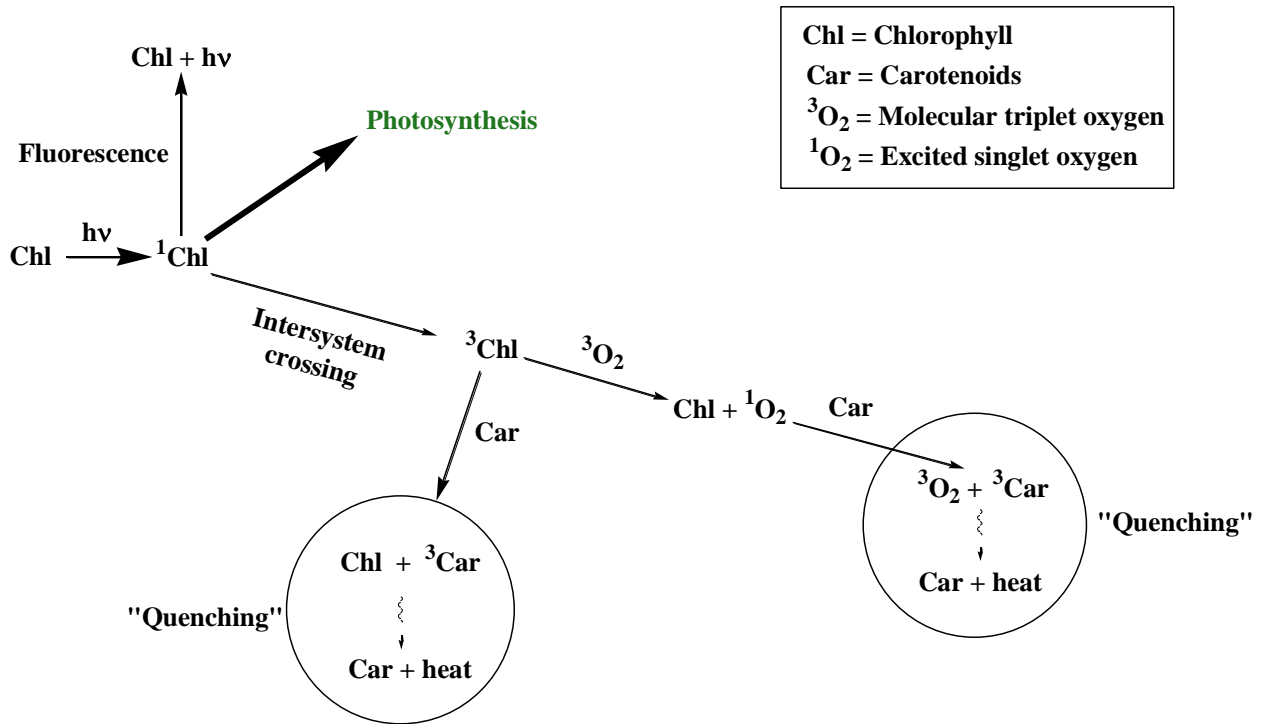


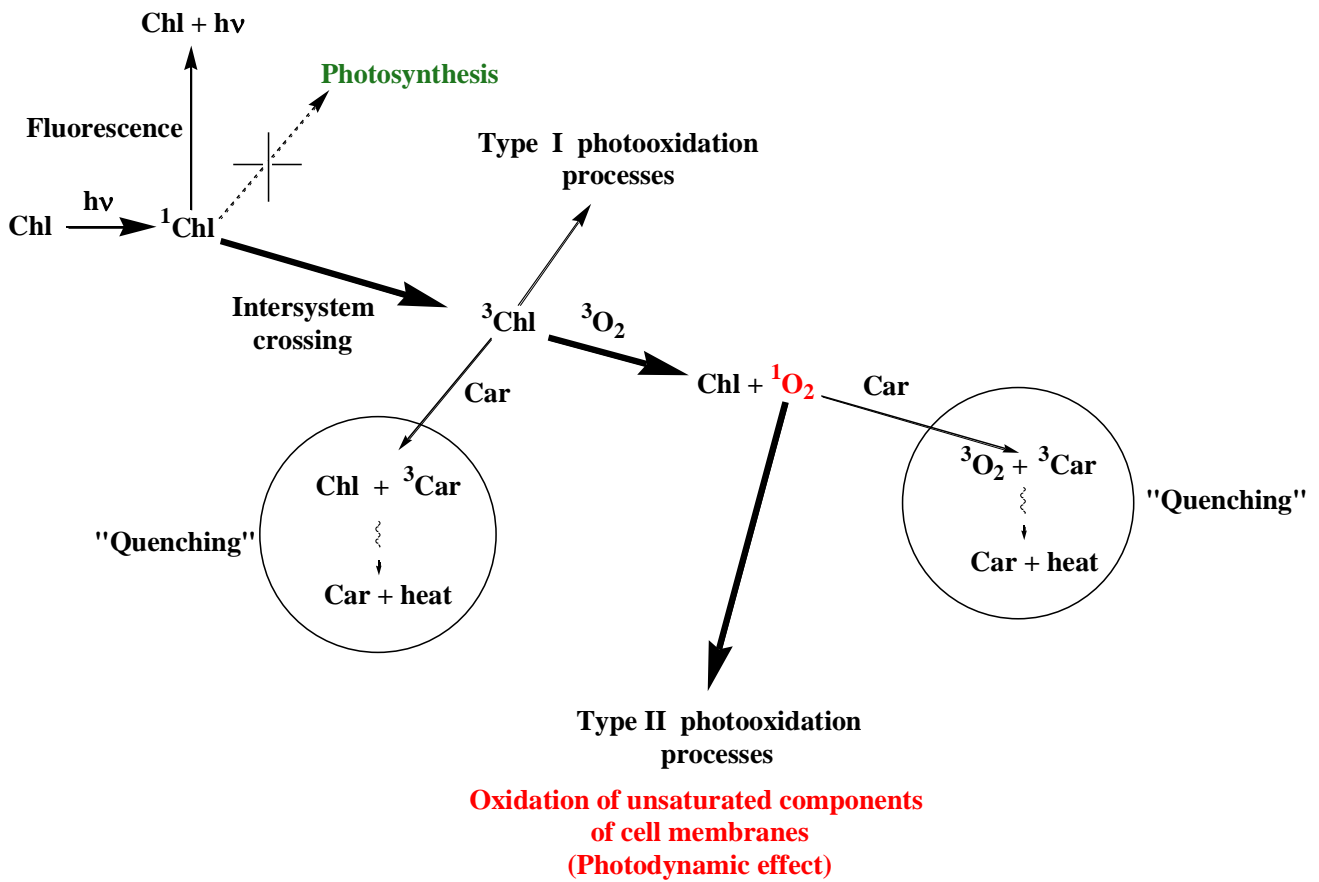
Figure 2

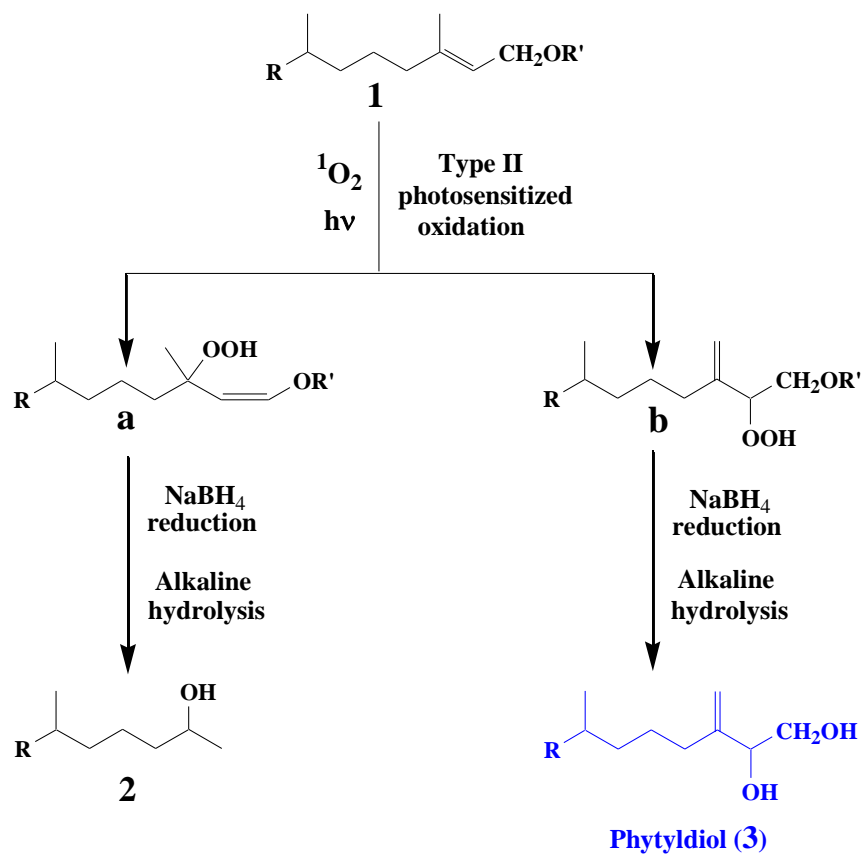
"Disclaimer: This is a pre-publication version. Readers are recommended to consult the full published version for accuracy and citation."

A

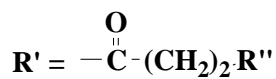
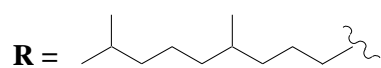


B





Tracer of chlorophyll photooxidation



$\text{R}'' =$ More or less oxidized tetrapyrrolic structure

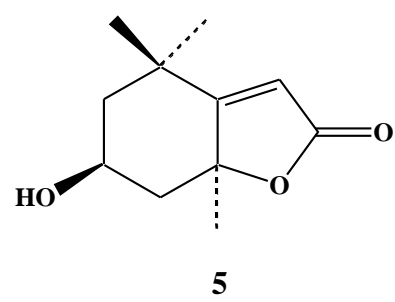
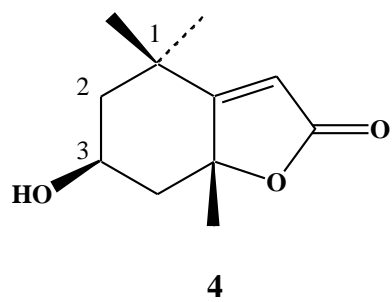


Figure 5

“Disclaimer: This is a pre-publication version. Readers are recommended to consult the full published version for accuracy and citation.”

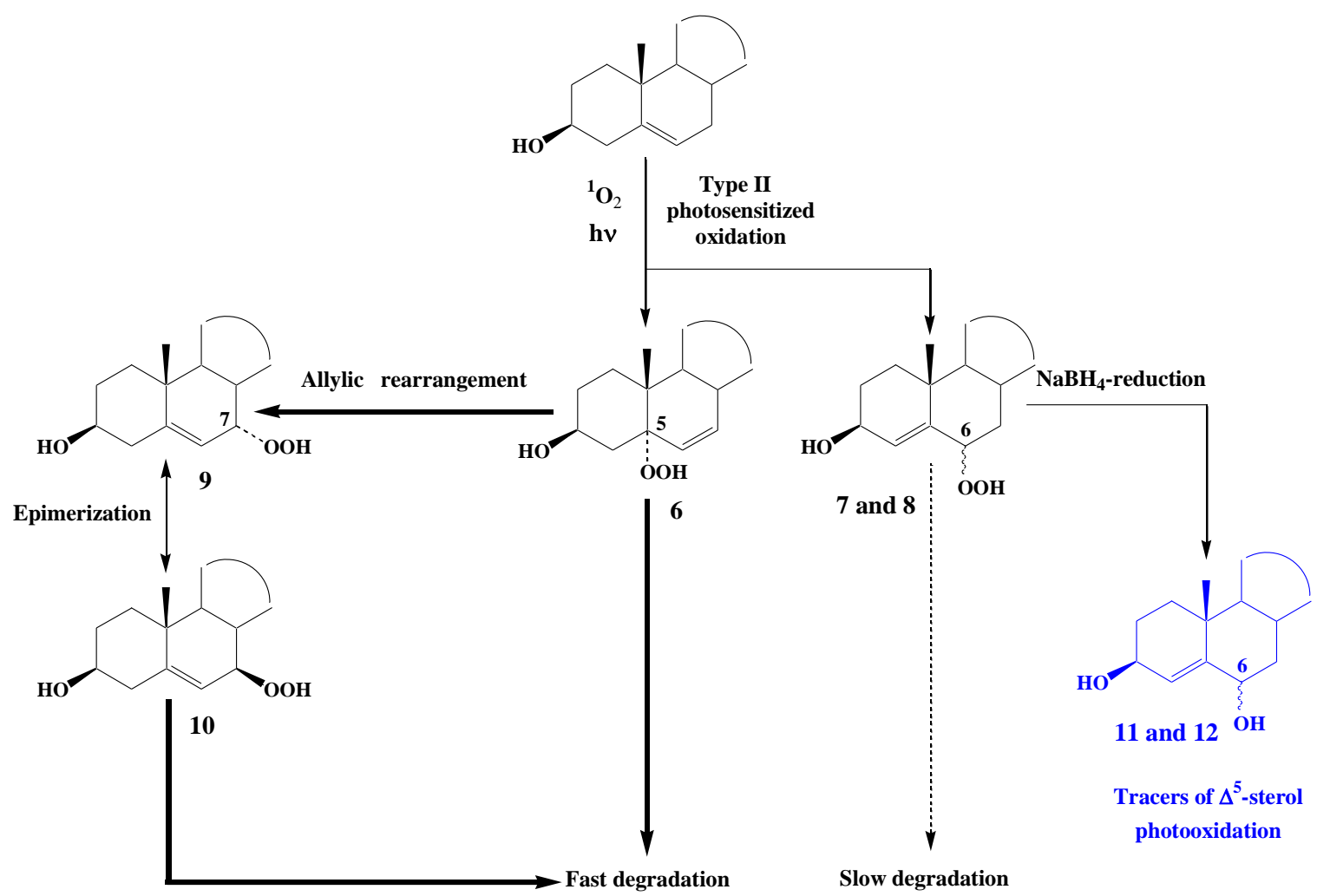
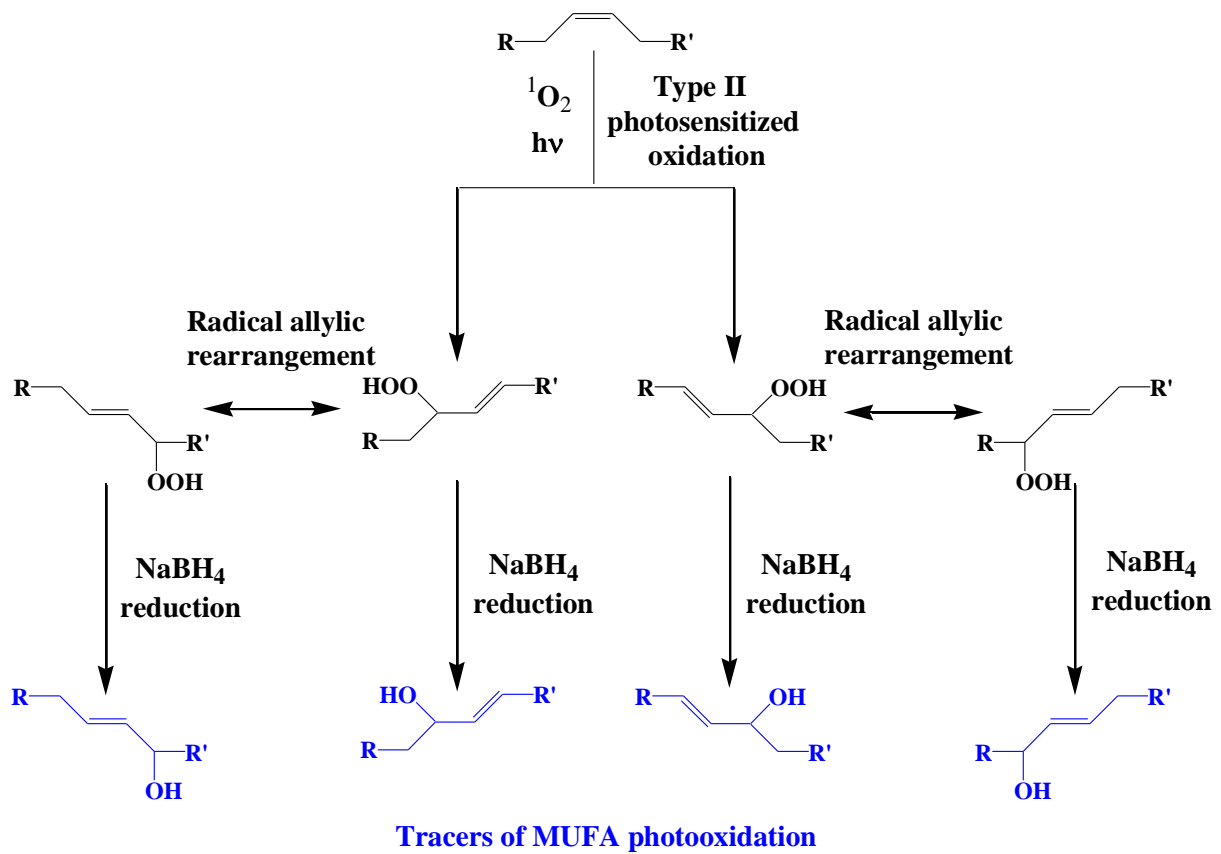


Figure 6

"Disclaimer: This is a pre-publication version. Readers are recommended to consult the full published version for accuracy and citation."



$\text{R} = -(\text{CH}_2)_n-\text{CH}_3$

$\text{R}' = -(\text{CH}_2)_m-\text{COOH}$

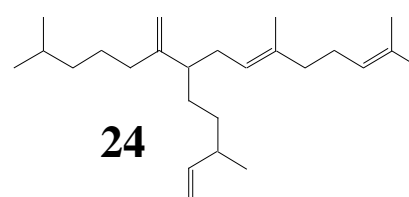
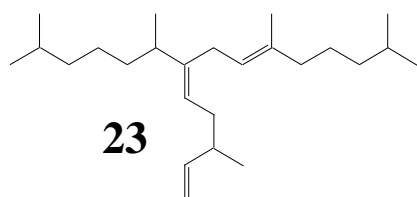
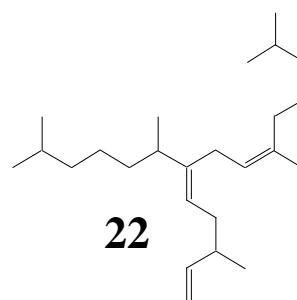
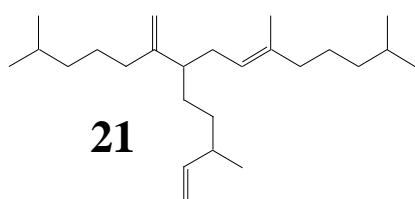
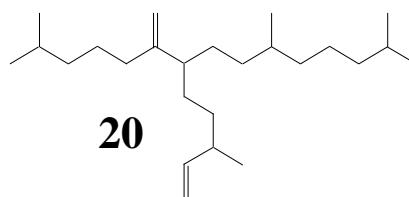
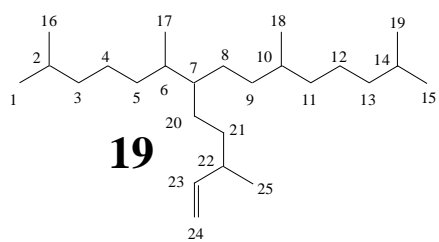
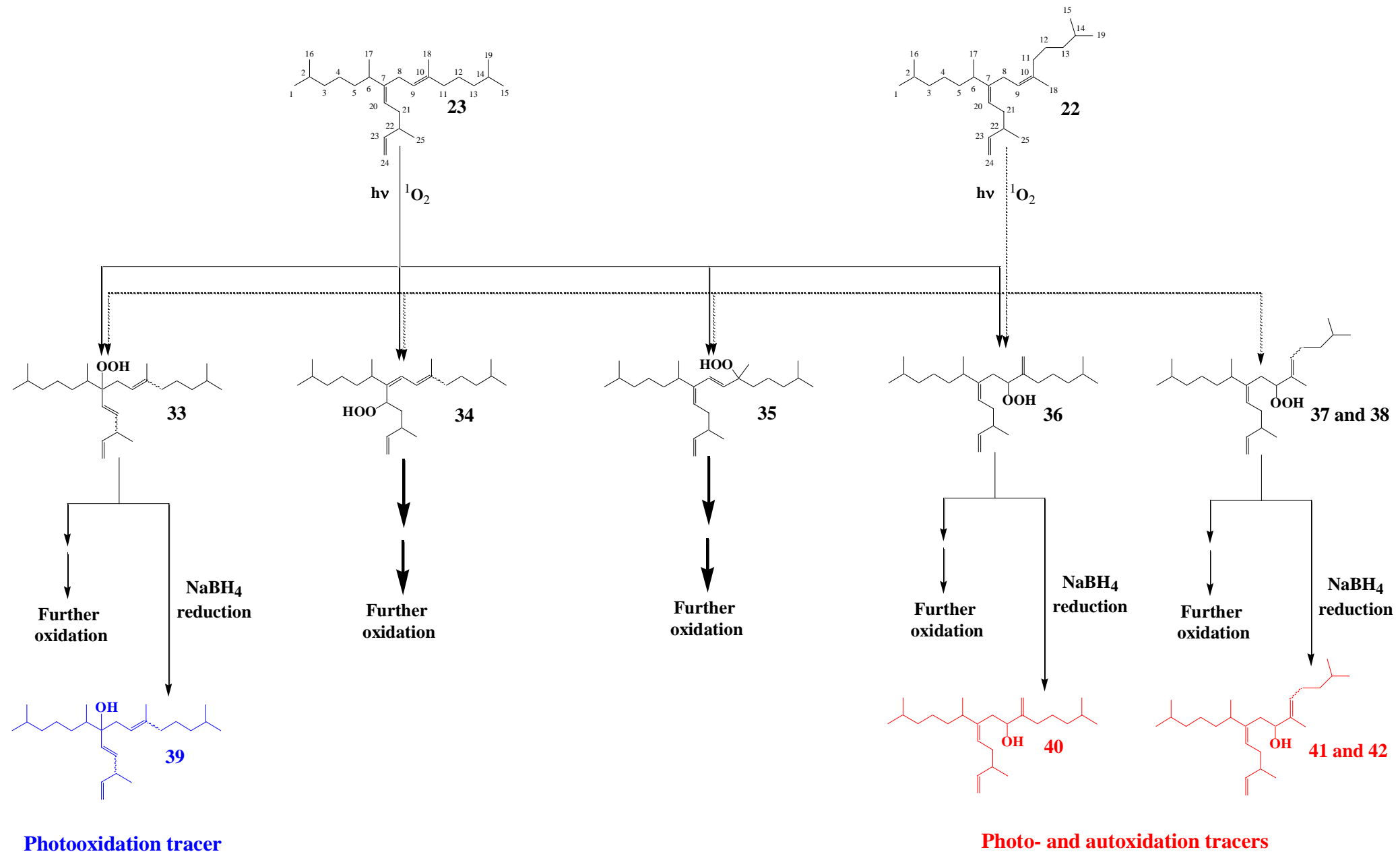


Figure 8

“Disclaimer: This is a pre-publication version. Readers are recommended to consult the full published version for accuracy and citation.”



Photooxidation tracer

Photo- and autooxidation tracers

Figure 9

"Disclaimer: This is a pre-publication version. Readers are recommended to consult the full published version for accuracy and citation."

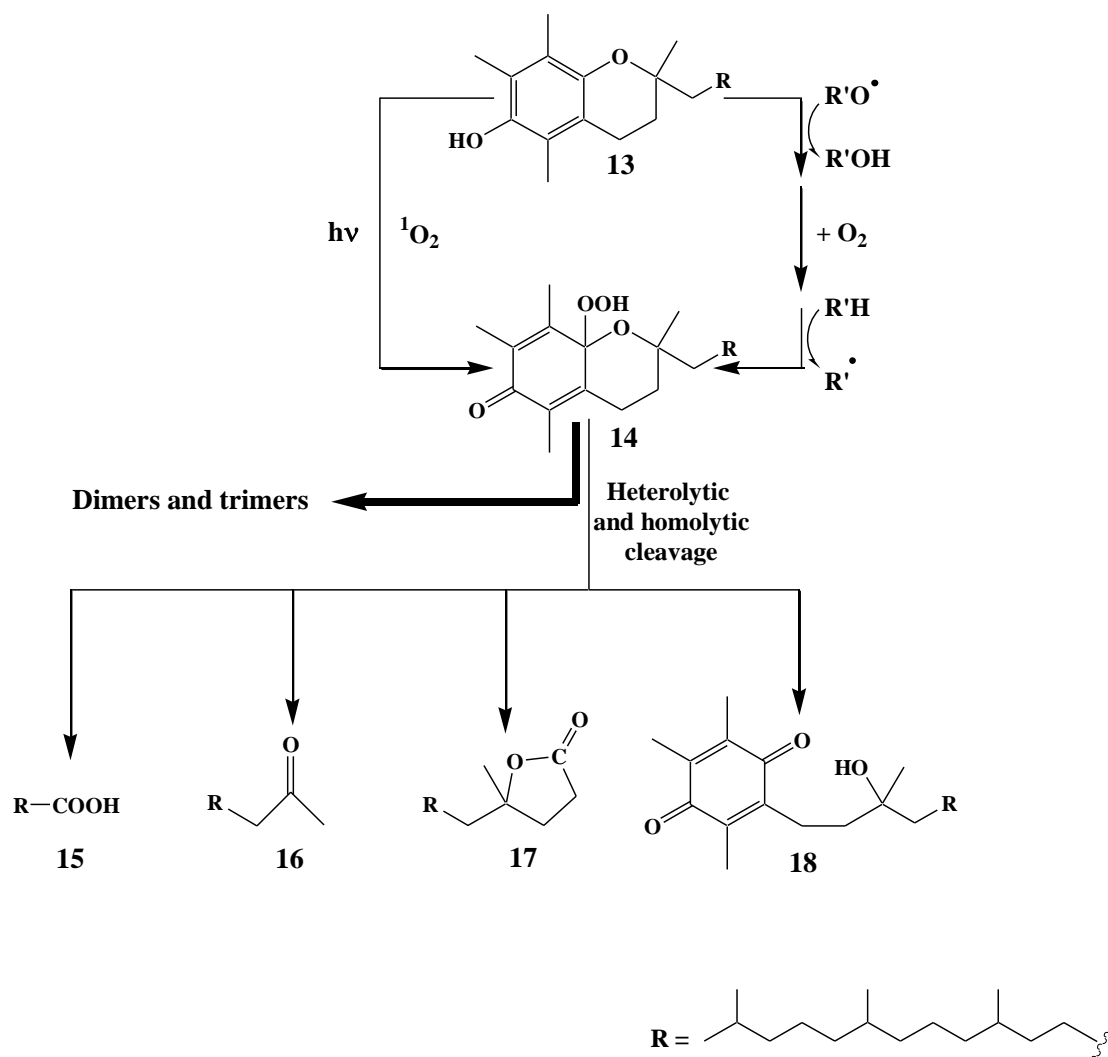
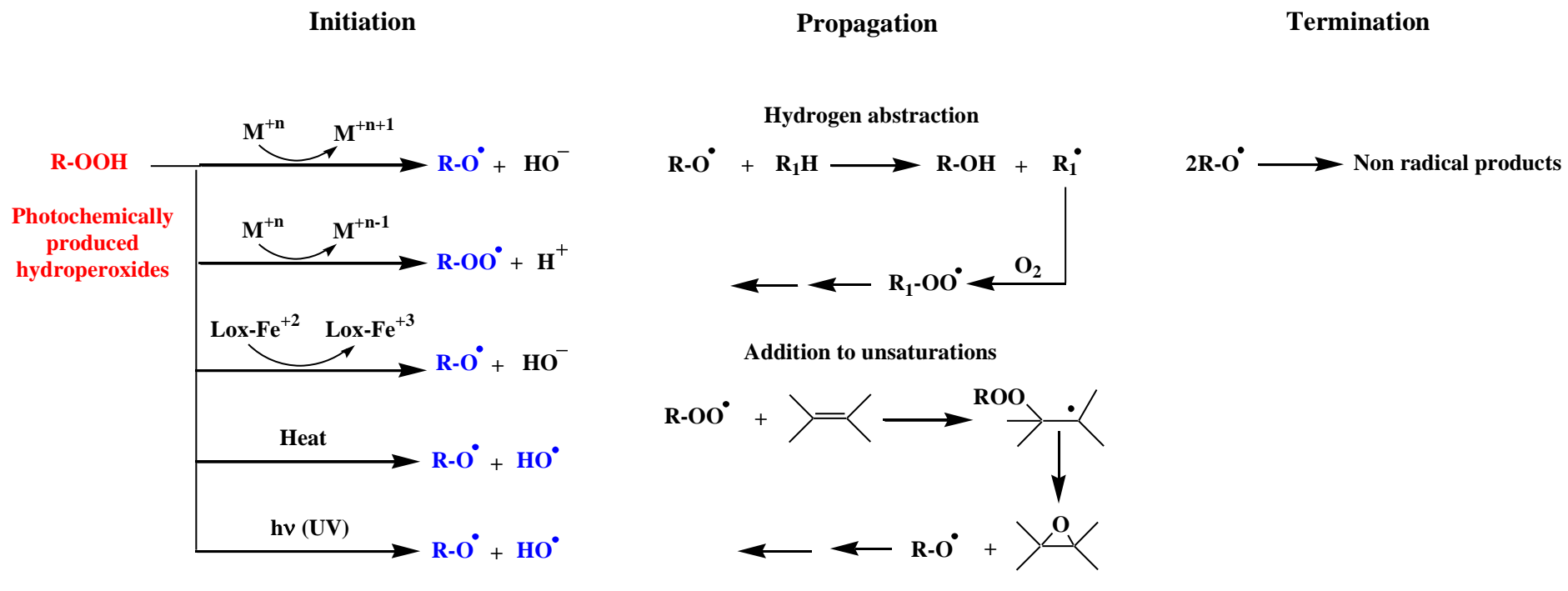


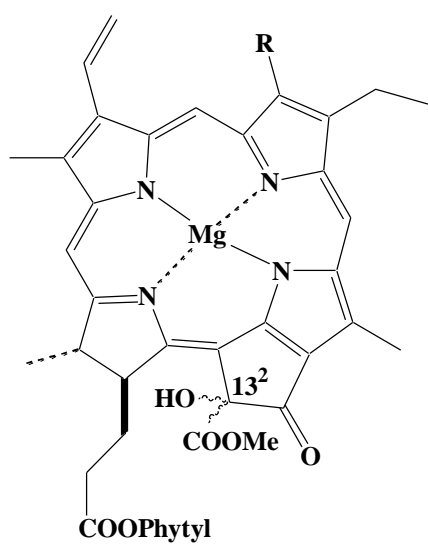
Figure 10

"Disclaimer: This is a pre-publication version. Readers are recommended to consult the full published version for accuracy and citation."



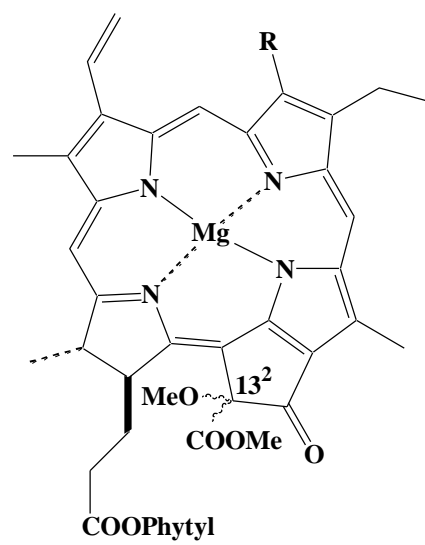
M = metal ion

Lox = Lipoxygenase



13²-Hydroxychlorophyll a

43



13²-Methoxychlorophyll a

44

Figure 12

"Disclaimer: This is a pre-publication version. Readers are recommended to consult the full published version for accuracy and citation."

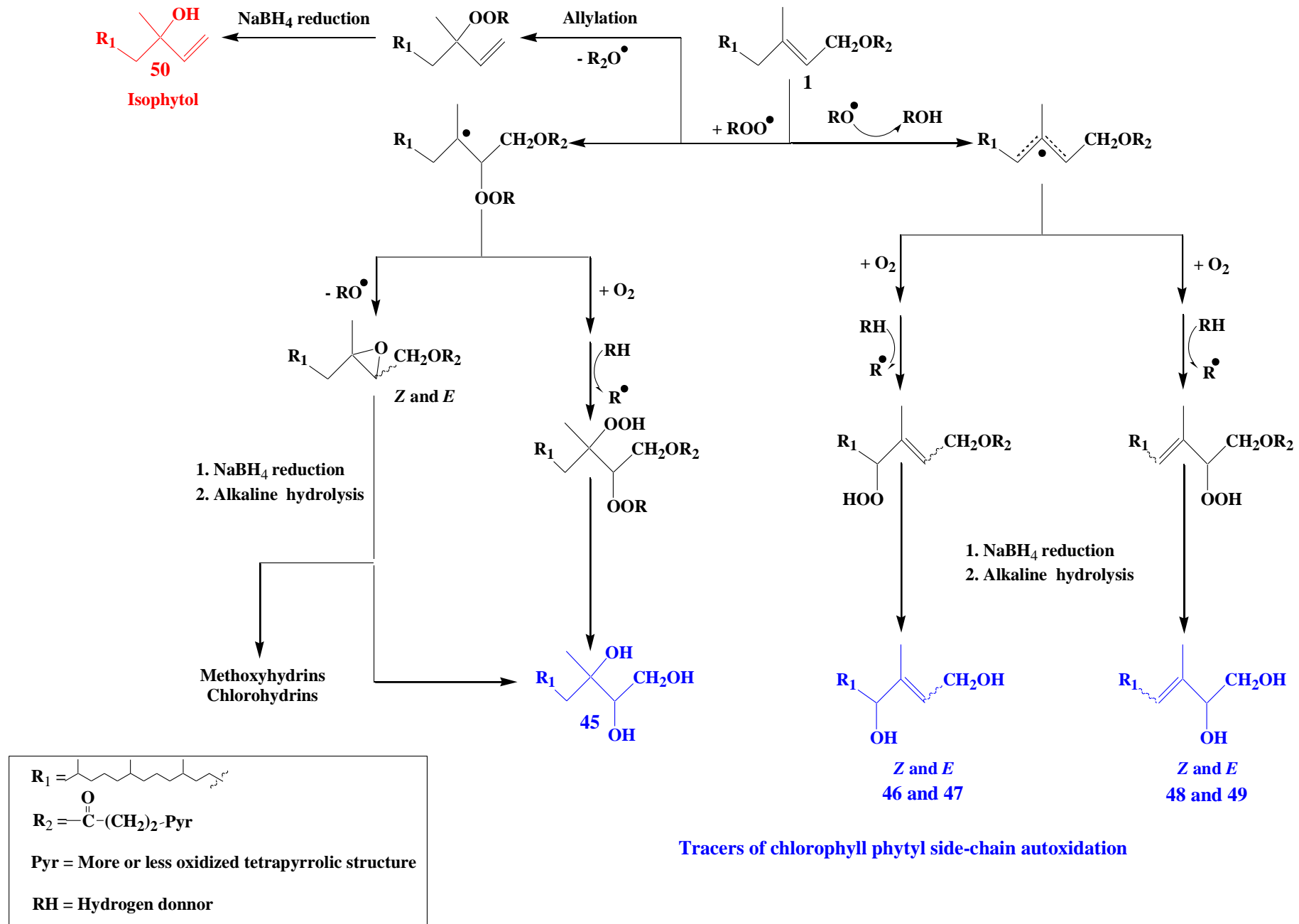
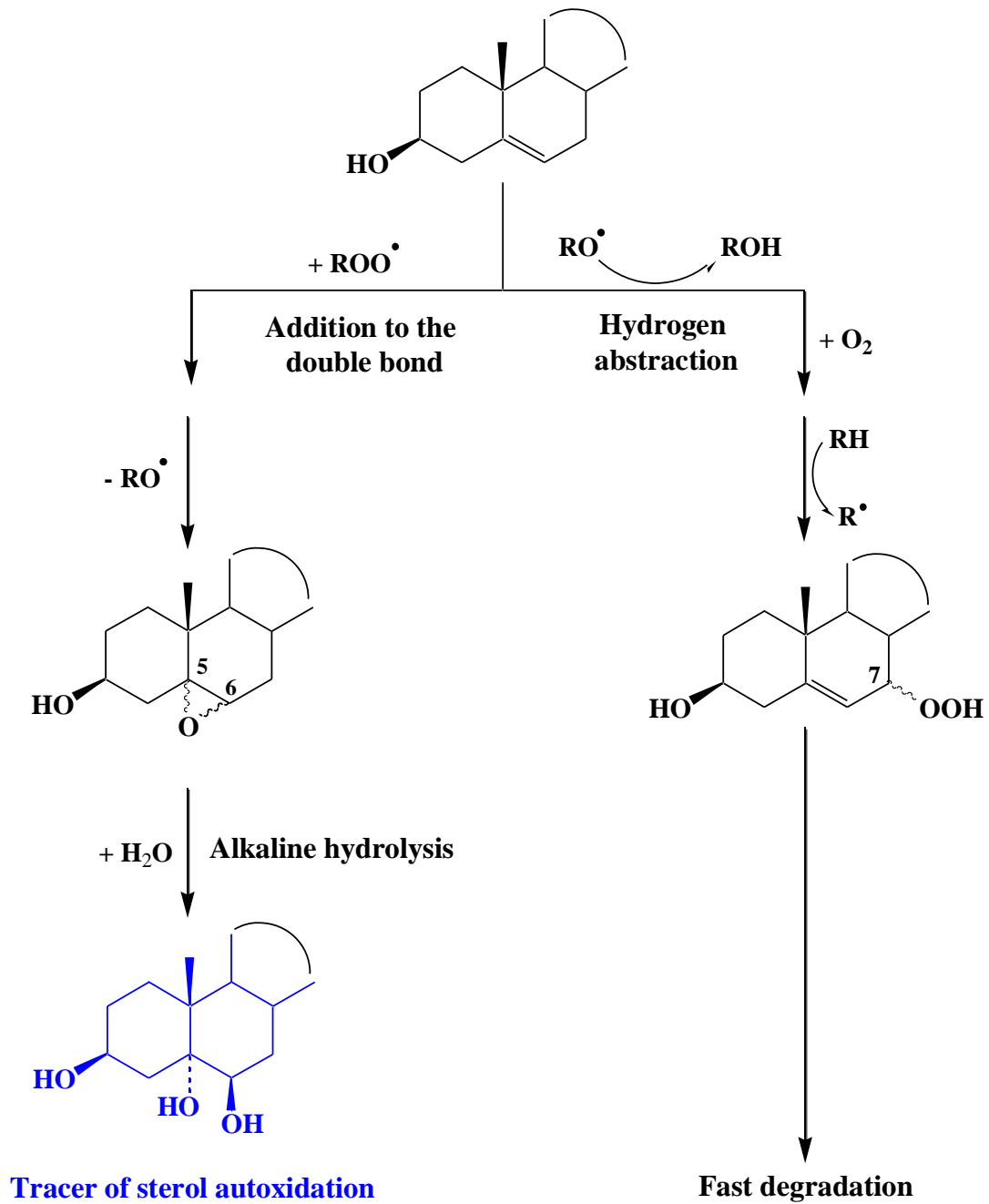
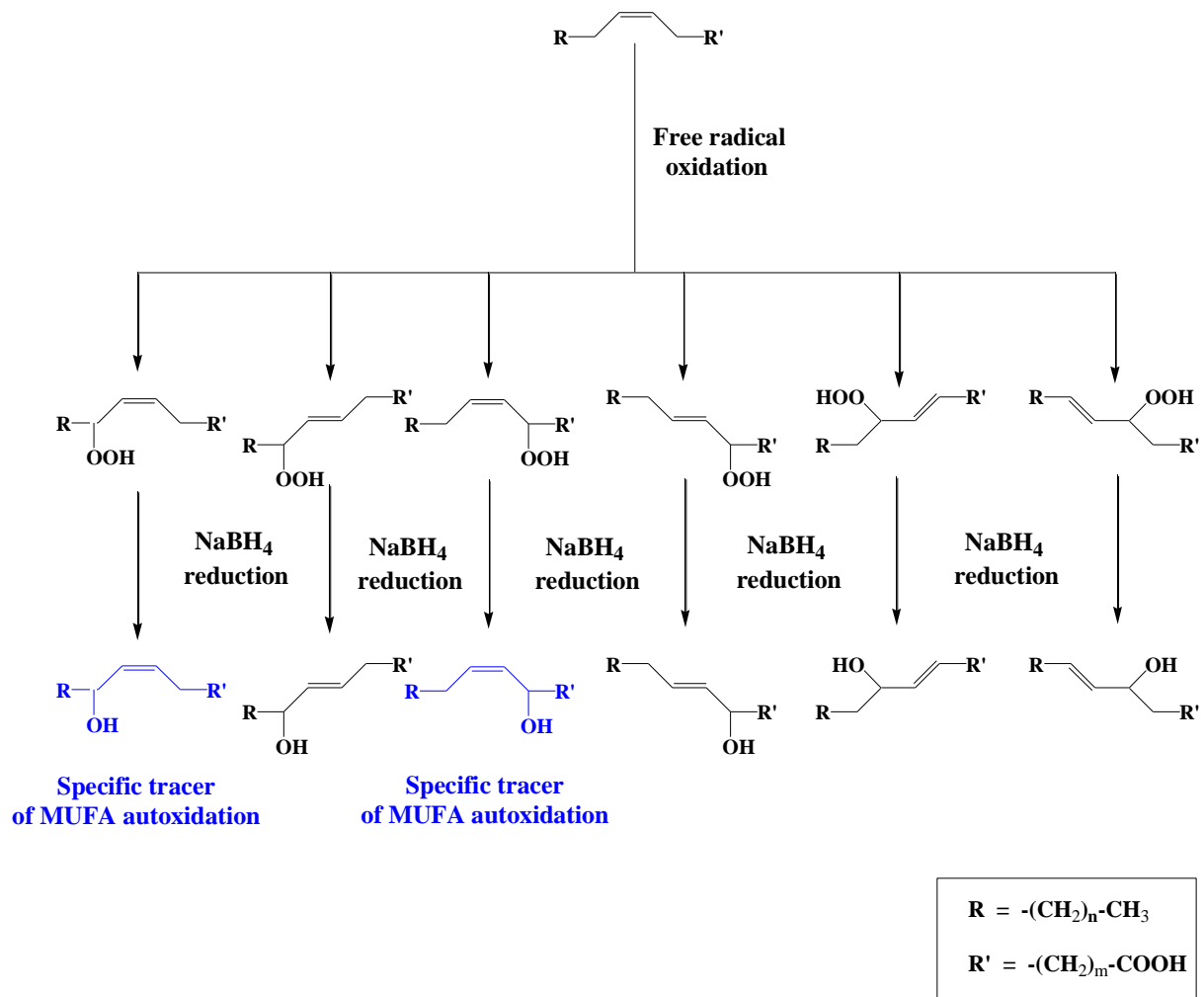
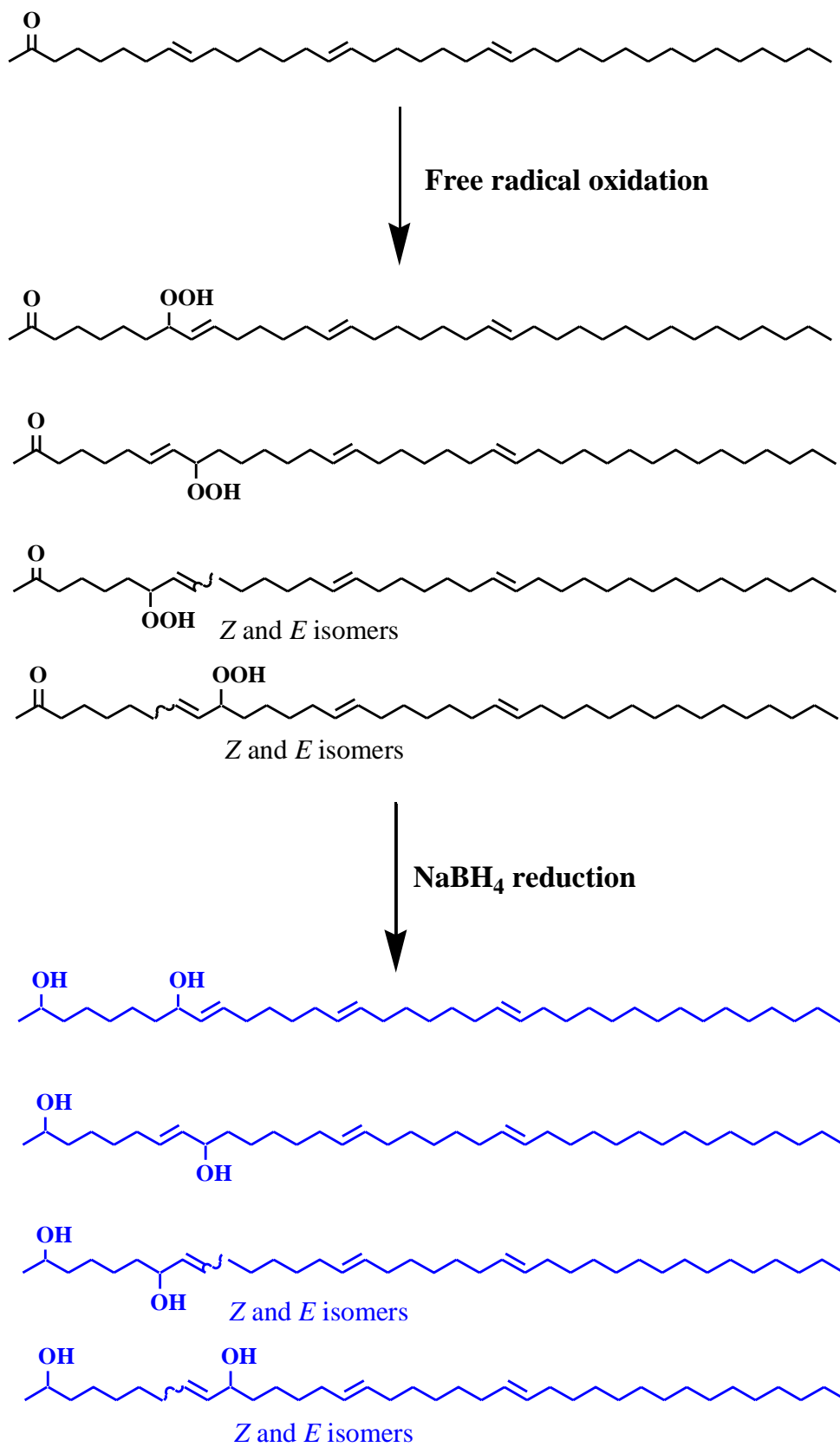


Figure 13

"Disclaimer: This is a pre-publication version. Readers are recommended to consult the full published version for accuracy and citation."



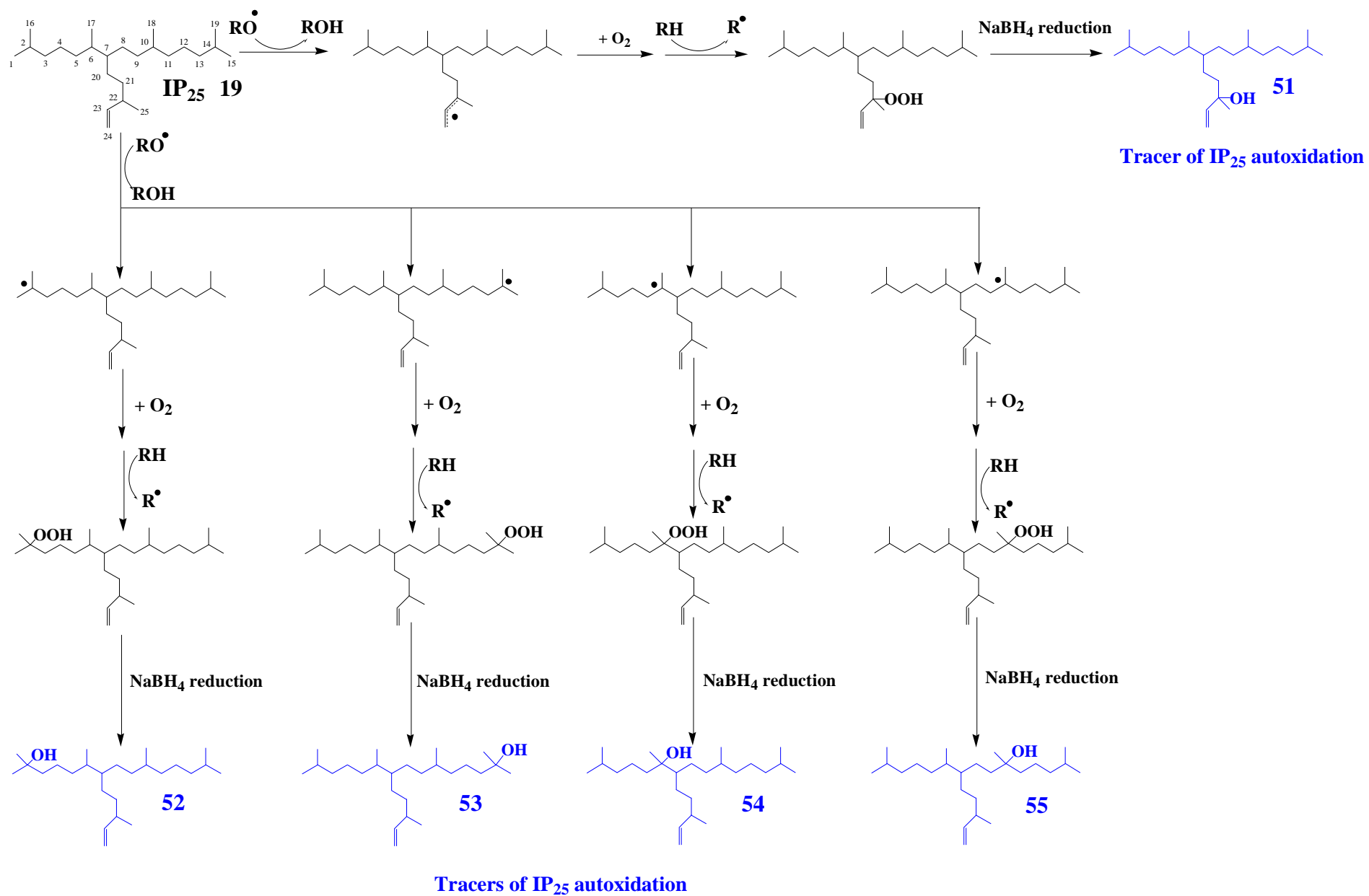




Tracers of alkenone autoxidation

Figure 16

"Disclaimer: This is a pre-publication version. Readers are recommended to consult the full published version for accuracy and citation."



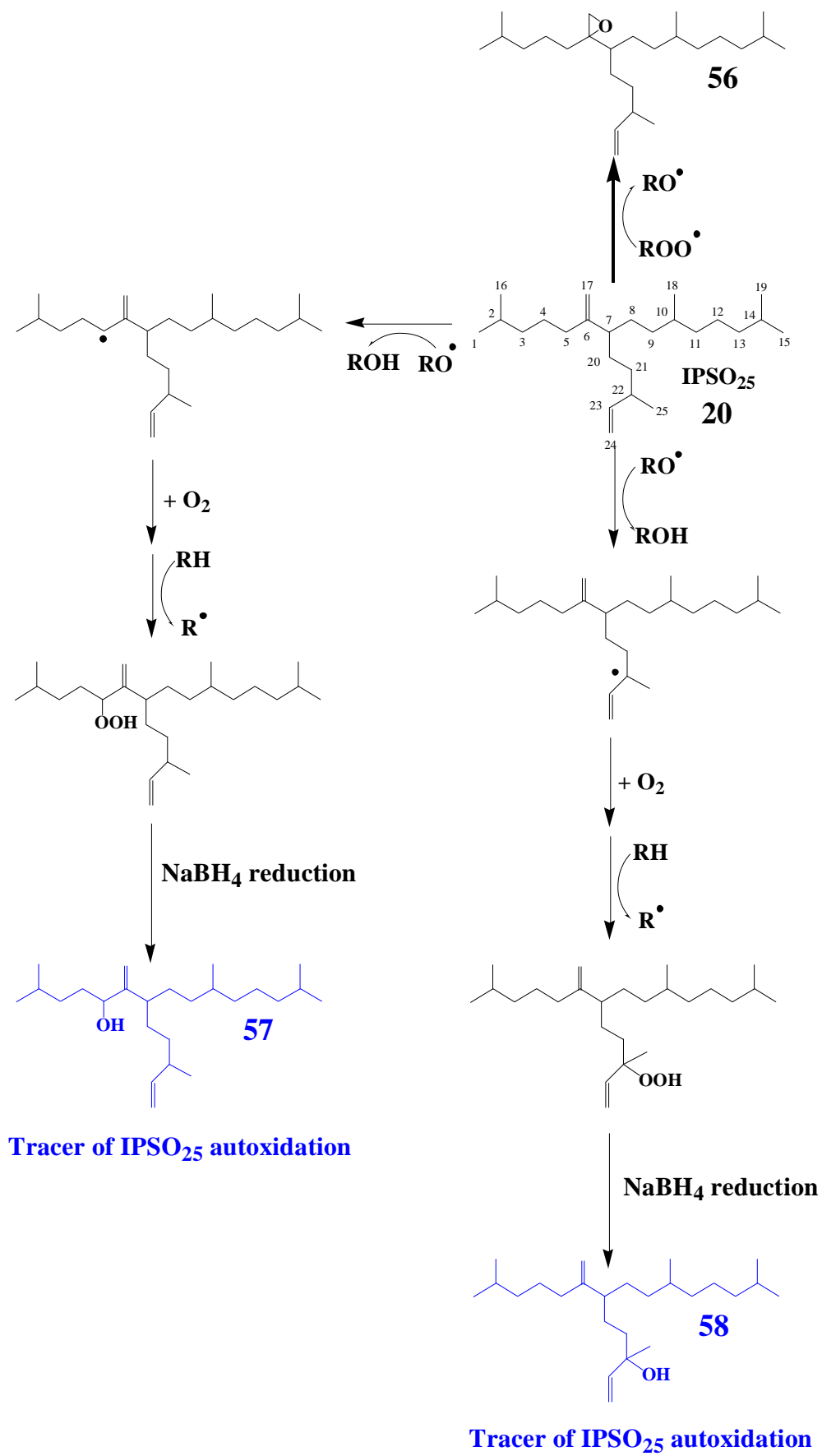


Figure 18

"Disclaimer: This is a pre-publication version. Readers are recommended to consult the full published version for accuracy and citation."

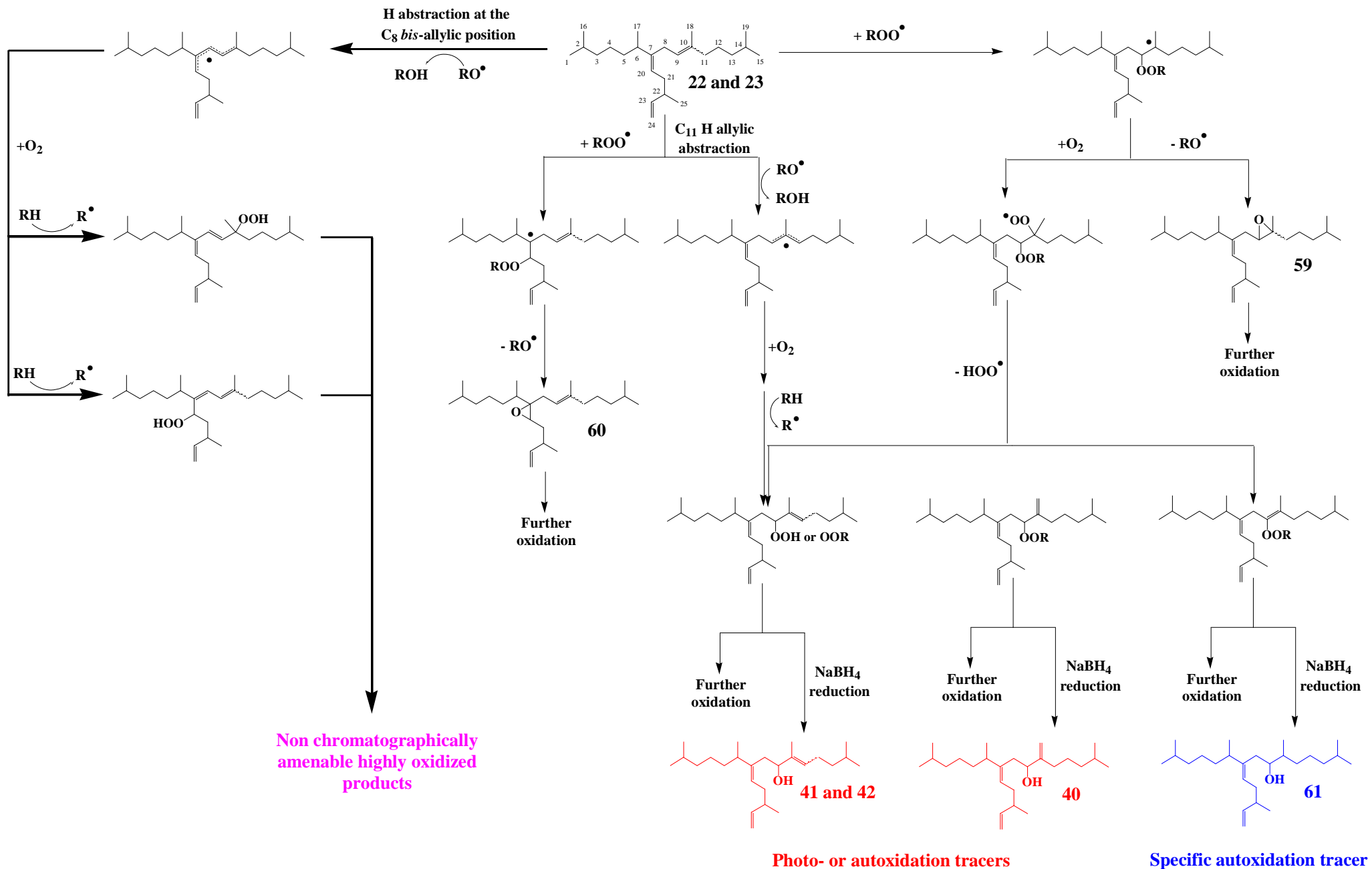


Table 1

Previous detection of algal lipid auto- and photooxidation products in natural samples.

Parent lipid	Autoxidation tracers	Photooxidation tracers	Sample type	Location	Autoxidation: Quantitative (Q) or qualitative (q) information	Photooxidation: Quantitative (Q) or qualitative (q) information	References
Alkenones	+		<i>Emiliana huxleyi</i>		q		Rontani et al., 2007a, 2013
	+		Sediments	Southeast Alaska	q		Rontani et al., 2013
	+		Sinking particles	Ligurian Sea	q		Rontani et al., 2007c
Chlorophyll		+	Sinking particles	Ligurian Sea		Q (10–100%)	Cuny et al., 2002; Marchand et al., 2005
			Suspended particles	Rhône River		Q (0–100%)	Galeron et al., 2015
			Suspended particles	Pacific Ocean		Q (20–70%)	Rontani et al., 2011
			Sinking particles	Pacific Ocean		Q (50–90%)	Rontani et al., 2011
			Suspended particles	Arctic		Q (0–50%)	Rontani et al., 2016
			Sinking particles	Arctic		Q (0–100%)	Rontani et al., 2012a, 2016
			Suspended particles	Antarctic		Q (3–50%)	Rontani et al., 2019a
		+	Sea ice	Arctic	q	Q (30–100%)	Rontani et al., 2014b
		+	<i>Posidonia oceanica</i>	Marseilles, France	q	Q (20%)	Rontani, 2019; Rontani and Galeron, 2016
			Terrestrial higher plants	Marseilles, France		Q (100%)	Rontani, 2019
	+	Microbial mats	Camargue, France	q		Rontani and Volkman, 2005	
	+	Phytoplankton	Antarctic	q		Rontani et al., 2014a	
Δ^5 -sterols		+	Sinking particles	Ligurian Sea		Q (0–30%)	Christodoulou et al., 2009
	+	+	Suspended particles	Rhône River	Q (10–90%)	Q (0–15%)	Galeron et al., 2015
	+	+	Suspended particles	Pacific Ocean	Q (0–30%)	Q (0–10%)	Rontani et al., 2011
	+	+	Sinking particles	Pacific Ocean	Q (0–30%)	Q (0–10%)	Rontani et al., 2011
	+	+	Sinking particles	Arctic	Q (0–20%)	Q (0–50%)	Rontani et al., 2012a, 2016

	+	+	Suspended particles	Arctic	Q (10–85%)	Q (0–30%)	Rontani et al., 2014d
		+	Suspended particles	Antarctic		Q (0–30%)	Rontani et al., 2019a
	+	+	Sea ice	Arctic	Q (0–50%)	Q (0–20%)	Rontani et al., 2014b
	+	+	Surface sediments	Arctic	Q (0–60%)	Q (0–40%)	Rontani et al., 2012b
		+	<i>Zostera noltii</i>	Arcachon, France		Q (100%)	Rontani et al., 2014c
		+	<i>Posidonia oceanica</i>	Marseilles, France		Q (70%)	Rontani, 2019
		+	Terrestrial higher plants	Marseilles, France		Q (30–50%)	Rontani, 2019
MUFAs	+	+	Sinking particles	Ligurian Sea	Q (0–50%)	Q (0–10%)	Marchand et al., 2005
	+	+	Suspended particles	Pacific Ocean	Q (0–11%)	Q (0–15%)	Rontani et al., 2011
	+	+	Sinking particles	Pacific Ocean	Q (0–5%)	Q (0–15%)	Rontani et al., 2011
	+	+	Sinking particles	Arctic	Q (0–70%)	Q (50–100%)	Rontani et al., 2012a; 2016
	+	+	Suspended particles	Arctic	Q (10–70%)	Q (5–50%)	Rontani et al., 2016
	+	+	Suspended particles	Antarctic	Q (0–90%)	Q (0–85%)	Rontani et al., 2019a
	+	+	Surface sediments	Arctic	Q (0–2%)	Q (0–5%)	Rontani et al., 2012b
HBI alkenes	+	+	Sea ice	Arctic	q	q	Rontani et al., 2014a
	+	+	Suspended particles	Antarctic	q	q	Rontani et al., 2019a
	+		Sediments	Arctic	q	q	Rontani et al., 2018; Rontani et al., 2019b
	+	+	Sympagic diatoms		q	q	Rontani et al., 2011, 2014d
Vitamin E	+	+	Sinking particles	Ligurian Sea	q	q	Rontani et al., 2007b
	+	+	Microbial mats	Camargue, France	q	q	Rontani and Volkman, 2005
	+	+	Haptophytes		q	q	Nassiry et al., 2009
	+	+	Sediments	Arctic	q	q	Belicka et al., 2002
	+	+	Sediments	German Bight	q	q	Schwartzbauer et al., 2000
	+	+	Soils	The Netherlands	q	q	Morley et al., 2005

Table 2Rate constants for reaction of $^1\text{O}_2$ with isolated acyclic double bonds in solvents.

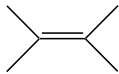
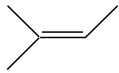

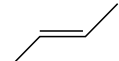
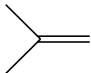
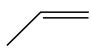
Substrate	k (mol ⁻¹ s ⁻¹)	References
	2.2×10^7	Hurst et al. (1985)
	7.2×10^5	Hurst et al. (1985)
	4.8×10^4	Hurst et al. (1985)
	7.2×10^3	Hurst et al. (1985)
	4.0×10^3	Hurst et al. (1985)
	2.3×10^2	Kopecky and Reich, 1965

Table 3

Comparison of photodegradation rates of HBI alkenes and other common lipids in pyridine in the presence of hematoporphyrin as sensitizer (adapted from Rontani et al., 2011, 2014a).

Compound	Code	1 st order degradation rate constant k (KJ ⁻¹ m ²)
C _{25:1} HBI (23-24) ^a (IP ₂₅)	19	1.7 × 10 ⁻⁵
C _{25:2} HBI (6-17, 23-24) (IPSO ₂₅)	20	1.1 × 10 ⁻⁴
C _{25:3} HBI (6-17, 9-10^b , 23-24)	21	1.6 × 10 ⁻²
C _{25:3} HBI (9-10(Z) , 7-20 , 23-24)	22	1.0 × 10 ⁻²
C _{25:3} HBI (9-10(E) , 7-20 , 23-24)	23	1.2 × 10 ⁻²
C _{25:3} HBI (5-6 , 9-10 , 23-24)	24	3.5 × 10 ⁻²
C _{25:4} HBI (6-17, 9-10 , 13-14 , 23-24)	25	3.7 × 10 ⁻²
C _{25:4} HBI (7-20 , 9-10(Z) , 13-14 , 23-24)	26	4.2 × 10 ⁻²
C _{25:4} HBI (7-20 , 9-10(E) , 13-14 , 23-24)	27	4.7 × 10 ⁻²
C _{25:4} HBI (2-3 , 7-20 , 9-10(Z) , 23-24)	28	4.3 × 10 ⁻²
C _{25:4} HBI (2-3 , 7-20 , 9-10(E) , 23-24)	29	5.1 × 10 ⁻²
Methyl oleate	30	1.2 × 10 ⁻³
Phytol acetate	31	1.0 × 10 ⁻³
Cholesteryl acetate	32	3.0 × 10 ⁻⁴
Vitamin E	13	1.9 × 10 ⁻²

^a Double bond positions (for carbon numbering see Fig. 6); ^b trisubstituted double bonds indicated in bold.

Table 4

Half-life doses ($D_{1/2}$) for visible light-dependent degradation of lipidic components in senescent phytoplanktonic cells*.

Compound	$D_{1/2}$ (Ein m ⁻²)
Chlorophyll a	1–4 ^{1,3}
Chlorophyll b	3–6 ^{1,2}
β-Carotene	1–2 ²
Sterols	8–64 ^{4,6}
Phytol	4–24 ^{1,4}
Mono-unsaturated fatty acids	14–23 ⁴
Di-unsaturated fatty acids	5–12 ⁴
Tri-unsaturated fatty acids	1–2 ^{4,8}
Di-unsaturated <i>n</i> -alkenes [#]	10–342 ⁷
Tri-unsaturated <i>n</i> -alkenes [#]	7–16 ⁷
Tetra-unsaturated <i>n</i> -alkenes [#]	2 ⁷
C _{37:2} Alkenone	346 ⁶
C _{37:3} Alkenone	231 ⁶
C _{25:3} HBI with one trisubstituted double bond	5 ⁸
IP ₂₅	950 ⁸

¹ Cuny et al., 1999⁴ Rontani et al., 1998⁷ Mouzdahir et al., 2001² Nelson, 1993⁵ Rontani et al., 1997a⁸ Rontani et al., 2011³ Rontani et al., 1995⁶ Rontani et al., 1997b

* Senescence obtained after several freeze-thaw cycles inducing some disruption of cellular structures (Nelson, 1993).

[#] With *cis* double bonds.[§] Estimated from relative photodegradation rate constants of IP₂₅ and C_{25:3} HBI in solvents (Rontani et al., 2011)

Table 5

Comparison of autoxidation rates of HBI alkenes and other common lipids in hexane in the presence of *tert*-butyl hydroperoxide and di-*tert*-butyl nitroxide at 65 °C under darkness (adapted from Rontani et al., 2014a).

Compound	Code	1 st order degradation rate constant k (h ⁻¹)
C _{25:1} HBI (23-24) ^a (IP ₂₅)	19	1.0 × 10 ⁻³
C _{25:2} HBI (6-17, 23-24) (IPSO ₂₅)	20	4.0 × 10 ⁻³
C _{25:3} HBI (6-17, 9-10 ^b , 23-24)	21	2.9 × 10 ⁻²
C _{25:3} HBI (9-10 (Z), 7-20 , 23-24) ^c	22	3.2 × 10 ⁻¹
C _{25:3} HBI (9-10 (E), 7-20 , 23-24) ^c	23	4.0 × 10 ⁻¹
C _{25:4} HBI (6-17, 9-10 , 13-14 , 23-24)	25	6.7 × 10 ⁻²
Methyl oleate	30	3.6 × 10 ⁻²
Phytyl acetate	31	2.1 × 10 ⁻²
Cholesteryl acetate	32	5.7 × 10 ⁻²

^a Double bond positions (for carbon numbering see Fig. 7); ^b trisubstituted double bonds indicated in bold; ^c presence of a bis-allylic position.